Plant Physiology Preview. Published on March 14, 2019, as DOI:10.1104/pp.19.00051

Short title: Tandem fluorescent protein timers for plants

Tandem fluorescent protein timers for non-invasive relative protein lifetime measurement in plants.

Hongtao Zhang[1*], Eric Linster[2*], Lucy Gannon[1], Wiebke Leemhuis[2], Chelsea A. Rundle[1], Frederica L. Theodoulou[1#], Markus Wirtz[2#]

1. Plant Sciences Department, Rothamsted Research, Harpenden, AL5 2JQ, UK
2. Centre for Organismal Studies, University of Heidelberg, Heidelberg 69120, Germany

* These authors contributed equally
# Co-corresponding authors

One-sentence summary: Tandem fluorescent protein timers enable non-invasive analysis of protein turnover in intact plant cells, allowing tests of how different genetic backgrounds and treatments affect protein stability.

Author contributions: HZ and LG constructed plasmids and transgenic plants, carried out immunoblot and confocal analysis of *Nicotiana benthamiana* and Arabidopsis, EL and WL carried out transient transformation of Arabidopsis and did protein lifetime measurements, CR did root measurements and provided technical support, MW and FLT conceived and directed the study, FLT drafted the manuscript. All authors read and approved the manuscript prior to submission.

Funding information: Research at Rothamsted was funded by the Biotechnology and Biological Sciences Research Council (BBSRC) through grant BB/J016276/1 and the Tailoring Plant Metabolism (TPM) Institute Strategic Grant BBS/E/C/000I0420. Research at Heidelberg was funded by the German Research Council (DFG) via the Collaborative Research Centre 1036 TP 13 and the European Union by the ERA-CAPS project KatNat.

Corresponding author emails: freddie.theodoulou@rothamsted.ac.uk; markus.wirtz@cos.uni-heidelberg.de

Abstract

Targeted protein degradation is an important and pervasive regulatory mechanism in plants, required for perception and response to the environment as well as developmental signalling. Despite the significance of this process, relatively few studies have assessed plant protein turnover in a quantitative fashion. Tandem fluorescent protein timers (tFTs) offer a powerful approach for the assessment of in vivo protein turnover in distinct subcellular compartments of single or multiple cells. A tFT is a fusion of two different fluorescent proteins with distinct fluorophore maturation kinetics, which enable protein age to be estimated from the ratio of fluorescence intensities of the two fluorescent proteins. Here, we used short-lived auxin signalling proteins and model N-end rule pathway reporters to demonstrate the utility of tFTs for studying protein turnover in living plant cells of *Arabidopsis thaliana* and *Nicotiana benthamiana*. We present transient expression of tFTs as an efficient screen for relative protein lifetime, useful for testing the effects of mutations and different genetic backgrounds on protein stability. This work demonstrates the potential for using stably expressed tFTs to study native protein dynamics with high temporal resolution in response to exogenous or endogenous stimuli.

Introduction

The protein content of cells is not static, but is modified constantly by the combined actions of protein synthesis and degradation, a process termed proteostasis. In recent years, protein breakdown has emerged as an important control mechanism that not only underpins the daily requirements of cellular maintenance but also permits responses to environmental stimuli and progression through different developmental stages. In eukaryotes, the primary pathway for targeted protein degradation is the ubiquitin/proteasome system (UPS). Around 6% of the proteins encoded by the *Arabidopsis thaliana* genome are dedicated to this process, underlining its importance in plants (Vierstra, 2009). In plants, the UPS has been shown to target intracellular regulators with central roles in hormone signalling, the regulation of chromatin structure and transcription, morphogenesis, the circadian clock, responses to the environment, self-recognition and defence against pathogens (Vierstra, 2009; Miricescu et al., 2018). Similarly, the broad importance of proteostasis in humans is exemplified by disease states associated with its dysregulation (Ciechanover, 2013). Proteasome-mediated protein degradation is complemented by autophagy and compartment-specific AAA+ proteases (Nelson et al., 2014; Nelson and Millar, 2015).

Much effort has been expended on analysing protein synthesis, particularly the role of transcription, which is readily quantified on a genome-wide scale using microarrays and RNA-seq. These techniques can also be used to identify RNAs that are actively translated via isolation of RNA from polysomes (Zanetti et al., 2005). However, it is generally accepted that the correlation between protein and mRNA abundance is imperfect (Schwanhäusser et al., 2011). Whereas dramatic improvements to proteomics technology mean it is now feasible to measure abundance changes in several thousands of proteins in a single experiment (Bensimon et al., 2012), measuring protein abundance in different genotypes or in response to a stimulus does not distinguish between protein synthesis and degradation. Therefore, specific approaches are required to quantify protein degradation.

Classically, protein turnover has been analysed using pulse-chase metabolic labelling followed by immunoprecipitation. Protein lifetimes have also been estimated using transgenic plants expressing luciferase reporter fusions in cycloheximide chase assays (Worley et al., 2000; Dreher et al., 2006). More recently, high accuracy mass spectrometry (MS) has been combined with metabolic labelling to determine the degradation kinetics of many proteins in parallel, with Single Reaction Monitoring MS offering improved sensitivity and selectivity for selected proteins of interest (Claydon and Beynon, 2012; Holman et al., 2016). Protein turnover can also be analysed systematically using pulsed or dynamic stable isotope labelling with amino acids in culture (SILAC), although such methods are restricted to cell or tissue cultures (Doherty et al., 2009; Schwanhäusser et al., 2011; Boisvert et al., 2012; Welle et al., 2016; Savitski et al., 2018). Although powerful, proteomics approaches lack cellular and subcellular resolution, are biased towards relatively abundant proteins, and the kinetics of metabolic labelling dictate a lower limit for the half-lives ($t_{1/2}$) that can be quantified (Nelson et al., 2014; Li et al., 2017). This effectively excludes many interesting proteins involved in signalling such as transcriptional regulators, which are typically of low abundance, may have high turnover rates and are often restricted to specific cell types. Moreover, a key feature of signalling pathways that cannot readily be captured in a proteomics workflow or an immunoprecipitation experiment is the movement of proteins between subcellular compartments. Intracellular trafficking and turnover of regulatory proteins such as transcription factors, transporters and E3 ligases play important roles in plant signalling and development (Friml, 2010; Gallagher et al., 2014; Habets and Offringa, 2014; Podolec and Ulm, 2018). In plants, intercellular movement of proteins and peptides is also important in development, for example in root differentiation, where key transcription factors traffic between different cell types (Lee et al., 2006; Long et al., 2015).

Fluorescent proteins (FPs) offer alternative means to study the dynamics of protein turnover with the additional benefit of spatial resolution and potentially high sensitivity. A number of approaches are possible. Photo-switchable FPs may be employed in microscopy-based pulse-chase experiments, whereby a pulse of local light irradiation generates an activated population of a protein species that can be followed in time and space. Alternatively, in a bleach-chase experiment, the protein removal rate can be determined after bleaching a subset of the fluorescently labelled protein population in a given cell (Eden et al., 2011). Both these types of experiments require a time course and fitting models to signal intensities in order to yield turnover estimates. In contrast, fluorescent timers change colour as a function of protein age, due to fluorophore maturation. A tandem fluorescent timer (tFT) is a fusion of two single-colour FPs that undergo fluorophore maturation with different kinetics, an arrangement that overcomes many of the disadvantages of early single FP timers (Khmelinskii and Knop, 2014; Khmelinskii et al., 2016). The ratio of slow-maturing FP to fast-maturing FP fluorescence intensities provides a measure of protein age through single time point imaging.

The tFT technology was originally developed in yeast (Khmelinskii and Knop, 2014; Khmelinskii et al., 2016) and has been used in animal systems (Dona et al., 2013; Barry et al., 2016; Alber et al., 2018; Durrieu et al., 2018) but despite its broad applicability, it has not yet been applied in plants. Studies combining stable isotope labelling with MS indicate that the degradation rates of plant mitochondrial proteins span more than a 50-fold range (Nelson et al., 2013) and a 100-fold range was reported for plastid proteins (Nelson et al., 2014), therefore different approaches will ultimately be required to cover the entire temporal range of plant protein degradation. The maturation rates of tFT fluorophores can be tuned to be appropriate for the half-lives of the proteins under investigation (Khmelinskii and Knop, 2014). Here, we focus on short-lived proteins, employing a timer composed of the fast-maturing monomeric green fluorescent protein superfolder GPF (sfGFP) and the slower maturing monomeric red fluorescent protein mCherry that was pioneered for use in yeast (Khmelinskii et al., 2016). We demonstrate that mCherry-sfGFP faithfully reports relative protein lifetime in plants using two exemplars: the N-end rule pathway and auxin signalling proteins. We show that transient expression of tFTs provides a rapid, straightforward method to compare the effects of mutations and different genetic backgrounds on protein stability and that the generation of stable lines expressing tFTs permits analysis of protein stability at subcellular resolution, in different cell types and in response to exogenous and endogenous stimuli.

Results

Proof of concept: establishing the measurement of relative protein lifetime using model N-end rule reporters

The range of protein ages that can be interrogated with a tFT depends upon the maturation kinetics of the respective FPs (Khmelinskii et al., 2012). Arabidopsis protein half-lives span a few minutes [e.g. auxin signalling proteins; (Worley et al., 2000; Ouellet et al., 2001; Dreher et al., 2006)] to many hours or even days (e.g. histones; Nelson et al., 2013; 2014). Whereas sfGFP matures with a half-time of ~6 min, mCherry maturation can be described by a two-step process with maturation half-times of ~17 min (first step) and ~30 min (second step) (Khmelinskii et al., 2012). This makes the mCherry-sfGFP timer suitable to study the degradation of proteins with half-lives between ~10 min and ~8h (Khmelinskii et al., 2012). First, we tested the integrity of the mCherry-sfGFP reporter in planta by fusing it to the C-terminus of the cytosolic, hexameric protein, SERINE ACETYLTRANSFERASE5 (SAT5; Wirtz et al., 2010) and transfecting *Nicotiana benthamiana* leaf epidermal cells. Free GFP and fluorescent protein dimers (e.g., mCherry-sfGFP) are well known to translocate into the nucleus (Seibel et al., 2007); however, SAT5-tFT was localised in the cytosol and clearly excluded from the nucleus (Fig. 1A). Immunoblotting indicated that the fusion protein was largely intact (Fig. 1B). Together, these results indicate that neither mCherry nor sfGFP was released from the fusion protein in vivo and that the tFT fusion faithfully reported the subcellular localisation of SAT5. We cannot fully exclude the possibility that an extremely short-lived sfGFP or mCherry-sfGFP fragment has been released from SAT5-tFT and is diluted in the nucleus to undetectable levels. However, such a theoretical and highly instable fragment would not interfere, in practice, with the lifetime measurement in planta.

We next designed a Gateway-based cloning scheme to generate plant transformation constructs for expression of proteins of interest fused at the C-terminus to the mCherry-sfGFP tFT, under the control of a promoter of choice. We created protein timers designed to be targeted for proteasomal turnover according to the Arg/N-end rule pathway for protein degradation (Fig. 2A). The N-end rule relates the half-life of a protein to its amino (N-) terminal residue (Bachmair et al., 1986). Substrates for this pathway are generated post-translationally by non-processive endopeptidase cleavage to reveal a new N-terminal amino acid residue or by a combination of co-translational and post-translational modifications of the N-terminus (Gibbs et al., 2011; Gibbs et al., 2014). Proteins bearing basic, bulky or hydrophobic N-terminal residues (classified as destabilising) are recognised by E3 ligases with different specificities and targeted for degradation by the proteasome (Potuschak et al., 1998; Varshavsky, 2011; Gibbs et al., 2014). In *Arabidopsis thaliana*, PROTEOLYSIS1

(PRT1) is an E3 ligase with specificity for aromatic amino acids, whereas PROTEOLYSIS6 (PRT6) targets basic N-terminal residues (Stary et al., 2003; Garzón et al., 2007; Mot et al., 2018). N-end rule substrates can also be created artificially by the ubiquitin fusion technique, in which a genetically-encoded N-terminal ubiquitin domain is cleaved in vivo by deubiquitinating enzymes to reveal a destabilising residue at the N-terminus (the so-called N-degron; Varshavsky, 2000; Fig. 2A). Timer constructs thus designed to release Arginine-tFT (R-tFT) and Phenylalanine-tFT (F-tFT) in planta were transiently introduced into wild type Arabidopsis (Col-0) and also the *prt6-5* and *prt1-1* mutants which lack E3 ligases specific for basic and aromatic N-termini, respectively (Garzón et al., 2007; Graciet et al., 2009). Methionine-tFT (M-tFT), which is not a substrate for PRT6 or PRT1, was used as a control. The X-tFT constructs were detected in the nucleus and cytosol (Supplemental Fig. S1). F-tFT and R-tFT were relatively unstable in wild type cells, with mCherry-sfGFP ratios of 0.35 $\pm$ 0.027 and 0.36 $\pm$ 0.009 respectively, compared to 0.85 $\pm$ 0.027 for M-tFT. In contrast, stability of the N-end rule reporters was increased significantly in the appropriate E3 ligase mutant background (Fig. 2B, C). Thus, the mCherry-sfGFP tFT enables quantification of protein stability in a transient expression system. The results also demonstrate that the lifetime of a tFT fusion can be dictated by a single amino acid change (in this case, at the N-terminus), indicating that fate of the mCherry-sfGFP component is influenced predominantly by the degron and not by intrinsic properties of the fluorescent protein fusion itself.

Transient systems typically afford high, potentially non-physiological protein expression levels. Therefore, we tested the performance of the X-tFT fusions in transgenic plants. Stable transgenic lines were established in Arabidopsis N-end rule mutant backgrounds and crossed to wild type (Col-0) plants to generate control lines harbouring the same transgene event. Lines were analysed by immunoblotting: signals corresponding to the expected molecular weight of R-tFT and F-tFT after cleavage of ubiquitin (60.5 kDa) were barely detectable in Col-0 but their abundance was increased by treatment with the proteasome inhibitor Bortezomib (Fig. 3A, B). Abundance of the reporter proteins was considerably higher in the N-end rule mutant backgrounds, *prt6-5* and *prt1-1*, with a modest further stabilisation by Bortezomib. A second protein species of approximately 45 kDa was detected with the GFP antibody, but not the mCherry antibody; this likely represents an mCherry cleavage product known to be formed during cell extract preparation (Gross et al., 2000; Shemiakina et al., 2012). Quantification of mCherry and sfGFP signals by confocal microscopy revealed that F-tFT and R-tFT were less stable than M-tFT in wild type roots, but the mCherry/sfGFP ratios were increased significantly by application of a second proteasome inhibitor, MG-132 (Fig. 3C, D). F-tFT and R-tFT were stabilised in the N-end rule mutants, *prt1-1* and *prt6-5*, respectively, relative to the wild type (Fig. 3C, D). Taken together, these data indicate that

the model N-end rule tFT reporters are turned over by the proteasome in an N-end rule-dependent manner, and that this turnover can be faithfully monitored using ratiometric fluorescence measurements.

Benchmarking tFTs with auxin signalling proteins.

We then validated the tFT technique using endogenous proteins whose lifetimes have been measured using established methods. Relatively few studies have systematically addressed protein lifetime measurement in plants, but regulated degradation of Aux/IAA transcriptional regulators mediated by TRANSPORT INHIBITOR RESPONSE1/AUXIN SIGNALLING F-BOX proteins (TIR1/AFBs) is well known to play a crucial role in auxin signalling and plant development (Abel et al., 1994; Worley et al., 2000; Gray et al., 2001; Ouellet et al., 2001; Dreher et al., 2006). Aux/IAA proteins form part of the early response to auxin and many are extremely short-lived, which enables silencing of the auxin signal once the primary response has been initiated (Abel et al., 1994). This protein family is ideal for challenging the tFT system, since degrons have been identified, different members of the Aux/IAA family vary in their degradation rates and degradation is influenced by exogenous application of auxin (Dreher et al., 2006). Domain II of Aux/IAA proteins physically interacts with TIR1/AFB and is required not only for rapid degradation but also the auxin-mediated acceleration of degradation (Gray et al., 2001; Ramos et al., 2001; Dharmasiri et al., 2005a; Dharmasiri et al., 2005b; Kepinski and Leyser, 2005; Dreher et al., 2006).

To benchmark the mCherry-sfGFP tFT, we tested three Arabidopsis Aux/IAA proteins with half-lives ranging from a few minutes to hours (Table 1). Initially, we employed transient expression in *N. benthamiana* leaf epidermis, a commonly used system for analysing fluorescent protein fusions, to compare the lifetimes of IAA17, IAA28 and IAA31-tFT fusions. Comparing the intensity of the mCherry and sfGFP signals in agro-infiltrated *N. benthamiana* leaves enabled a straightforward ranking of protein lifetime (indicated by the slopes of the scatter plots), with the rank order IAA17≤IAA28<IAA31, consistent with the literature (Fig. 4; Table 1). Introduction of the P88L mutation which recapitulates a Domain II lesion in the Arabidopsis *axr3-1* auxin signalling mutant (Rouse et al., 1998; Ouellet et al., 2001) significantly increased the stability of IAA17-tFT (Fig. 4B). This result demonstrates the utility of transient expression of mutant or truncated proteins in *N. benthamiana* for the rapid analysis of degrons and other structural factors that influence turnover.

To quantify protein stability and test the effect of exogenous auxin, IAA-tFTs were transiently expressed in Arabidopsis. In agreement with previous studies (Tao et al., 2005; Arase et al.,

2012), IAA17-tFT was localised predominantly in the nucleus, with some signal present in the cytosol. Apparently, the cytosolic pool of IAA17-tFT was less stable than nuclear-localised IAA17-tFT (Fig. 5A). Treatment with the synthetic auxin, 2,4-dichlorophenoxy acetic acid (2,4-D) reduced the mCherry/sfGFP ratio of nuclear IAA17-tFT from 0.819 ± 0.063 to 0.302 ± 0.042 and reduced the cytosolic mCherry signal to below the limit of detection. As in *N. benthamiana*, the lifetime of $IAA17_{P88L}$-tFT was considerably longer than that of IAA17-tFT in Arabidopsis and was not significantly influenced by auxin treatment (Fig. 5A, B). In Arabidopsis leaf epidermal cells, the stability of IAA28-tFT was similar to that of IAA17-tFT whereas IAA31-FT was longer-lived. Auxin treatment reduced the lifetime of both proteins (Fig. 5A, B) and removal of auxin receptor function in the *tir1-1 afb2* mutant (Dharmasiri et al., 2005b) resulted in stabilisation of IAA28-FT (Fig. 5C, D). This indicates that turnover of the protein is dependent on canonical auxin signalling.

IAA-tFT stable lines report auxin dynamics

IAA17 and IAA28 play important roles in root growth and development, where their abundance is regulated by auxin (Leyser et al., 1996; Worley et al., 2000; Gray et al., 2001; Rogg et al., 2001; De Rybel et al., 2010; Sato et al., 2015). To explore the behaviour of IAA-tFT fusions in roots, Arabidopsis stable transgenic lines were established. Seedlings of lines expressing IAA17-tFT and IAA28-tFT under the control of the strong, semi-constitutive *CaMV35S* promoter were morphologically similar to wild type plants. However, $IAA17_{P88L}$-tFT roots exhibited an agravitropic phenotype (Supplemental Fig. S2), in agreement with the report of Swarup et al. (2005) that ectopic expression of $IAA17_{P88L}$ (the *axr3-1* gain of function mutant) in root epidermis blocked gravitropism. Two of the highest expressing IAA31-tFT lines had significantly fewer lateral roots than the wild type seedlings (Supplemental Fig. S3) consistent with the phenotype of plants over-expressing the untagged protein (Sato and Yamamoto, 2008). Collectively, these results demonstrate that the consequences of IAA-tFT fusion protein expression are similar to those of ectopically expressing untagged IAA proteins. Immunoblot analysis revealed that the IAA-tFT fusion proteins were largely intact (Fig. 6), therefore we tested the effect of manipulating auxin levels on IAA-tFT stability. As judged by immunoblotting, application of 2,4-D to seedlings reduced the abundance of IAA17-tFT, IAA28-tFT and IAA31-tFT, but not $IAA17_{P88L}$-tFT (Fig. 6).

Next, seedlings were examined by confocal microscopy, to assess protein stability in different regions of the root. It was difficult to detect sfGFP or mCherry signals in IAA17-tFT lines under control conditions, but $IAA17_{P88L}$-tFT gave a strong nuclear signal that was

297 evident throughout primary root tips and the differentiation zone (Supplemental Fig. S4).
298 Similarly, IAA28-tFT was difficult to detect in control conditions, although Bortezomib
299 treatment resulted in stabilisation (Supplemental Fig. S5). In contrast, IAA31-tFT was
300 detected in the nucleus and cytoplasm of primary root tips (Supplemental Fig. S4A) with the
301 stability apparently reflecting the prevailing auxin gradient (Supplemental Fig. S4B). IAA31-
302 tFT was also stabilised by Bortezomib treatment (Supplemental Fig. S5). Application of 2,4-D
303 to roots grown on vertical plates shortened the lifetime of IAA31-tFT (Fig. 7A). During
304 gravitropism-induced root curvature, auxin accumulates asymmetrically, dependent on the
305 root zone undergoing curvature. (Ottenschläger et al., 2003; Swarup et al., 2005; Laskowski
306 et al., 2008; Brunoud et al., 2012). We hypothesised that, in the differentiation zone, the
307 auxin minimum on the underside of a root undergoing gravitropism would lead to stabilisation
308 of IAA proteins and the auxin accumulation on the upper side of the root bend would reduce
309 the lifetime of IAA-tFT (Laskowski et al., 2008). Accordingly, rotation of seedlings to induce
310 bending resulted in an increase in the mCherry-sfGFP ratio of IAA31-tFT on the inside of the
311 root bend and a decrease on the outside (Fig. 7B). As expected, the lifetime of the auxin
312 non-responsive $IAA17_{P88L}$-tFT did not differ at the site of natural root bends (Supplemental
313 Fig. S4C). Thus, the IAA-tFT transgenic lines demonstrate that the mCherry-sfGFP fusion
314 accurately reports the effects of endogenous and exogenous signals on protein turnover in
315 vivo.
316
317
318 **Discussion**
319
320 ***The mCherry-sfGFP timer is degraded by the proteasome and reports plant protein***
321 ***dynamics***
322
323 Given the importance of proteostasis in plant physiology, accessible methods to monitor and
324 quantify protein turnover in time and space are of great utility, particularly for short-lived
325 proteins involved in signalling. Classical methods for measuring turnover of a specific protein
326 of interest are technically challenging, in part due to the requirement to treat tissue with the
327 global protein synthesis inhibitor, cycloheximide, which not only constitutes a severe stress
328 but is also difficult to apply in conjunction with a given stimulus and may not penetrate
329 tissues in a uniform manner. tFTs offer an alternative, non-invasive approach to assess
330 protein turnover in real time, in vivo. In this study, we employed model N-end rule reporters
331 and endogenous Aux/IAA proteins to test the suitability of FTs for reporting relative protein
332 lifetime in plants.
333

The synthetic reporters, R-tFT and F-tFT were released from the respective ubiquitin-X-mCherry-sfGFP fusions and as predicted, were subject to N-end rule-mediated proteasomal degradation in both transient and stable systems. Similarly, the IAA-tFT fusions exhibited a range of lifetimes and were stabilised by proteasome inhibitors. Both the artificial (X-tFT) and native (IAA-tFT) fusion proteins were longer-lived in transiently transformed Arabidopsis than the stable lines, potentially reflecting the higher expression levels typically achieved in transient expression systems, which may overload the proteasome. However, the relative stability of the test proteins in different genetic backgrounds was the same for transient and stable systems. Although strongly influenced by structural features, the half-life of a protein is not an intrinsically fixed property but depends on the protein's environment (Nelson et al., 2014; Nelson and Millar, 2015). For example, IAA turnover has been investigated by three different methods: immunoprecipitation from [^{35}S]-methionine-labelled seedlings, constitutive expression of luciferase fusions in stable Arabidopsis transgenic plants and a synthetic degradation assay in yeast (Ouellet et al., 2001; Dreher et al., 2006; Moss et al., 2015; Table 1). The reported half-lives vary 10-fold for IAA17 and ~2-fold for IAA28, suggesting that this parameter may be influenced by ectopic expression. In this proof-of-concept study, we employed a strong constitutive promoter, to facilitate the development of imaging parameters, but in the future, it will be instructive to generate stable lines expressing the protein-of-interest-tFT fusions under the control of native promoters to analyse protein degradation in the most relevant physiological context.

Incomplete proteasomal degradation has been reported for GFP-containing tandem timer combinations in yeast (Khmelinskii et al., 2016), but this was not observed in stable Arabidopsis lines expressing ubiquitin-X-tFT fusions or IAA-tFT fusions. This may reflect differences in proteasome processivity between species (Kraut et al., 2012). A ~45 kDa cleavage product detected by anti-GFP antibodies in extracts from plants expressing the F-tFT and R-tFT constructs was also observed previously in yeast and has been proposed, based on structural considerations, to arise from cleavage of mCherry during sample preparation (Gross et al., 2000; Khmelinskii et al., 2016). Importantly, exclusion of SAT5-tFT from the nucleus provides strong evidence that GFP is not cleaved from the mCherry-sfGFP tFT in planta, indicating that this tandem timer combination is a robust tool for assessing protein lifetime in plants.

The N-terminus is a determinant of protein stability in plants

Our results provide direct evidence for the relevance of the free N-terminal amino acid residue for plant protein stability, demonstrating that this feature can be recognised by distinct E3 ligases (Varshavsky, 2011; Gibbs et al., 2016). Whereas several studies have shown that the *abundance* of both artificial and selected endogenous proteins is dictated by the N-end rule in plants (Potuschak et al., 1998; Garzón et al., 2007; Gibbs et al., 2011; Licausi et al., 2011), tFTs show directly that *protein turnover* is influenced by the N-terminus, complementing lifetime measurements performed using tFT or classical cycloheximide chase methods in yeast and human systems (Varshavsky, 2011; Khmelinskii et al., 2012). The potential importance of the N-terminal amino acid for protein stability has also been shown in context of the acetylation (Ac)/N-end rule branch in yeast and plants for a limited number of proteins (Hwang et al., 2010; Xu et al., 2015; Linster and Wirtz, 2018), though the pathway is more nuanced and complex than originally envisaged in yeast (Kats et al., 2018). N-terminal modification of plant proteins is a dynamic and stress-induced process that, in turn, controls environmental stress responses via modulation of protein stabilities (Linster et al., 2015; Vicente et al., 2017). The combination of the ubiquitin fusion technique with the tFT sensor to release proteins with a defined N-terminus enables testing the importance of selective translation initiation or N-terminal modifications on turnover of the candidate protein in a fast and cost-effective manner, and also provides information of the subcellular localisation of the protein species. Furthermore, commercially available selective affinity matrices for GFP and RFP can be combined with the tFT tag in a dual affinity pull-down approach to directly link the relevance of post-translational modifications to an in vivo determined turnover rate for a candidate protein.

IAA-tFT fusions as an exemplar for studying protein lifetime in vivo

Following the positive results with artificial N-end rule reporters, we tested whether the stability of endogenous Aux/IAA proteins could also be determined using tFTs. Auxins act as an adaptor for binding Aux/IAA proteins to the F-box proteins TIR1 and AFB1-AFB5, which are components of $SCF^{TIR1/AFB}$ ubiquitination E3 complexes (Gray et al., 2001). Formation of the $SCF^{TIR1/AFB}$ complex leads to polyubiquitination and degradation of Aux/IAA proteins (Calderón Villalobos et al., 2012). Accordingly, degradation of IAA28-tFT was inhibited in the *tir1-1 afb2* mutant which markedly impairs but does not eliminate the auxin response (Dharmasiri et al., 2005b). Domain II of the Aux/IAA proteins contains a well-characterised degron, and the P88L mutation in this motif significantly increased the lifetime of the IAA17-tFT fusion, consistent with pulse-chase studies of ^{35}S-labelled IAA17 and the phenotype of the *iaa17*/*axr3-1* mutant (Rouse et al., 1998; Ouellet et al., 2001). Of the three IAA family

members tested, IAA31 was the longest-lived. Interestingly, Domain II is incompletely conserved in IAA31 (Dreher et al., 2006), containing Asp in place of a conserved Gly, comparable to Gly to Glu substitutions found in dominant mutants *shy2-3*/*iaa3* and *iaa18-1* (Tian and Reed, 1999; Reed, 2001). In agreement with the literature, exogenous application of auxin to stably transformed lines increased IAA-tFT turnover as did manipulation of endogenous auxin by induction of root bending, demonstrating that the system is able to resolve dynamic alterations in protein turnover in vivo. This will offer the possibility to explore micro-environments with locally altered protein stability in future studies. Also, although tFTs were developed as a protein age sensor, the success of the Domain II (DII)-Venus auxin sensor (Brunoud et al., 2012) suggests that fusion of Aux/IAA proteins or their degrons to mCherry-sfGFP has the potential for the development of second-generation auxin sensors. Finally, tFTs have been used to great effect in yeast-based high-throughput screens to understand mechanisms controlling protein turnover (Khmelinskii et al., 2012; Kats et al., 2018). $IAA17_{P88L}$-tFT provides a proof of concept for extending this approach to plants, for example by high throughput screening of EMS-mutagenised lines expressing a protein of interest fused to a fluorescent timer.

Conclusions and future perspectives

We have demonstrated two complementary tandem timer approaches to study plant proteostasis: a transient expression system for rapid assessment of protein turnover and a stable expression system for analysis of protein stability in near-native contexts. The transient system is straightforward and accessible to any lab with a confocal microscope, requiring only standard filters and laser settings for detection of GFP and RFP. Many applications can be envisaged, such as analysis of degrons by mutagenesis and deletion strategies, or using loss of function lines to test candidate substrates for the ~1400 E3 ligases in Arabidopsis, the majority of which have not been characterised (Vierstra, 2009; Hua and Vierstra, 2011). The transient system also provides a rapid means to screen new fluorescent protein combinations to extend the lifetime range of the system or to produce timers with different spectral properties. Stable expression of tFTs offers an even wider range of potential applications. The tFTs are particularly valuable for measuring processes out of steady-state, such as signalling events, which are difficult to address using fluorescent switchers (Knop and Edgar, 2014). In contrast to fluorescent switchers, tFTs do not require a physical intervention and can be imaged in single snapshots, which allows analysis of protein-turnover with high temporal resolution in a specimen. Consequently, analysis of protein turnover in response to a stimulus such as hormone or light treatment is

straightforward, and future development of quantitative imaging protocols will enable even more sophisticated approaches, for example, combining stably-expressed t-FTs with time-lapse imaging in tractable systems such as the Arabidopsis root (Larrieu et al., 2014) to explore and quantify protein turnover events during growth and development. Although fluorescent timers have generally been used to analyse proteasome-dependent protein turnover, in principle, they can be adapted to study autophagy or targeted to organelles such as mitochondria and plastids which have different degradation machineries (Nelson and Millar, 2015). tFTs have also been developed to study organelle division and partitioning in yeast (Kumar et al., 2018).

In summary, tFTs fill an unmet need for a simple, versatile method to quantify dynamic changes in plant protein stability using live imaging with high spatial and temporal resolution. tFTs provide the basis for development of a suite of sophisticated tools to study the fascinating and extensive plasticity of the plant proteome.

Materials and Methods

SAT5 construct

Full-length SAT5 (AT5G56760) was amplified from *Arabidopsis thaliana* leaf cDNA using the SAT5-tFT_For and SAT5-tFT_Rev primers by PCR, and fused with the tFT tag that was PCR-amplified from pMaM17 (Khemelinski et al., 2012) using the mCherry_For and sfGFP_Rev primers (Supplemental Table S1). The resulting SAT5-tFT fusion was cloned in the pBinAR vector to allow expression under control of the *CaMV35S* promoter. Correct integration of SAT5-tFT in the pBinAR-SAT5-tFT vector was verified by sequencing.

N-end rule and IAA reporters

For N-end rule reporters, the Ubi-X-mCherry-sfGFP cassette was amplified from p415-GAL1-Ubi-R-mCherry-sfGFP (pMaM107; Khmelinskii and Knop, 2014) using primers AttB1_ubi-X-tft_For and AttB2_ubi-X-tft_stop and recombined into plasmid pDONR221 to create an entry cassette. F- and M- variants were constructed by site-directed mutagenesis, using a QuikChange II XL kit (Agilent Technologies, UK) according to manufacturer's instructions. The different entry vectors were then recombined into pB2GW7 (Karimi et al., 2002). For IAA reporters, the mCherry-sfGFP cassette was amplified using primers AttB2r_mCsfGFP_For and AttB3_mCsfGFP_stop and recombined into plasmid pDONRP2R-P3 to create an entry cassette pEN-R2-mCsfGFP-L3. IAA17 (At1g04250), IAA28 (At5g25890) and IAA31

(At3g17600) were amplified from an Arabidopsis root cDNA library by PCR using the primers in Supplemental Table S1 and recombined into plasmid pDONR221 to create entry vectors. $IAA17_{P88L}$ was generated by site-directed mutagenesis, using a QuikChange lightning kit. Vectors were sequenced to verify the presence of the mutation and to confirm that no unwanted mutations had been introduced. Each IAA entry vector pEN-L1-IAA-L2 was then recombined with pEN-L4-2-R1,0 (Karimi et al., 2007) and pEN-R2-mCsfGFP-L3 into pB7m34GW,0 (Karimi et al., 2005) to create constructs to express IAA-mCherry-sfGFP under the control of the *CaMV35S* promoter. Stable *Arabidopsis thaliana* transgenic lines were obtained by floral dip (Clough and Bent, 1998). Col-0 was transformed with the IAA-tFT constructs. *prt6-5* (Graciet et al., 2009) and *prt1-1* (Potuschak et al., 1998) were transformed with pHT23 (R-tFT) and pHT25 (F-tFT) respectively. Independent lines were crossed to Col-0 to obtain the same transgene events in the wild type background.

Growth of plants and treatments

Arabidopsis thaliana plants were grown for 5 weeks on soil or 7 d on 0.5 x MS containing 1% (w/v) sucrose and 0.6% (w/v) Phytagel under short day (8 h light) at 22°C during light and 18°C during night. For the application of 2,4-D or MG-132 to stably transformed Arabidopsis seedlings, the seedlings were grown for 7 d on 0.5 x MS medium solidified with agar and then transferred to 0.5 x MS medium supplemented with 5 µM 2,4-D or 50 µM MG-132 for 4 h. 2,4-D and MG-132 were dissolved in 0.1% (v/v) ethanol or 0.1 % (v/v) DMSO, respectively, with solvent only used as controls. For the Bortezomib treatment, 7-d-old seedlings were transferred to 0.5 x MS medium supplemented with 50 µM Bortezomib or DMSO for 24 h. Gravity-induced root bending was achieved by 180-degree rotation of the 14-d-old seedlings stably expressing IAA31-tFT grown on 0.5 x MS supplemented with 1% (w/v) sucrose and 0.6% (w/v) Phytagel. For treatment of transiently transformed Arabidopsis plants, the leaves were detached from intact plants at day four after the infiltration with *Agrobacterium* harbouring the construct of choice and were fed via the petiole for two hours with 100 µM 2,4-D dissolved in water. Ethanol dissolved in water served as control for the petiole feeding.

Arabidopsis transformation and confocal microscopy

Agrobacterium tumefaciens-mediated transient transformation of 5-week-old soil-grown Arabidopsis plants was performed according to Mangano et al. (2014). The transiently transformed plants were analysed four days after infiltration. Leaves were placed on a water-covered slide and analysed using a Nikon A1 confocal microscope equipped with Gallium

arsenide phosphide (GaAsP) detectors and solid-state lasers for excitation at 405, 488 and 561 nm. The fluorescence signal was imaged at 525/50 nm after excitation at 488 nm for sfGFP, and at 595/50 nm after excitation at 561 nm for mCherry. The laser power of 488 nm and 561 nm lasers were set to a one to three ratio. The spectral properties of mCherry and sfGFP are shown in Fig. S6. Ratiometric quantification of fluorescence images was performed after applying a Gaussian blur with a sigma of 1 and background subtraction in IMAGEJ (v.1.52h; https://imagej.nih.gov/ij). To produce a ratio image on a pixel by pixel basis, signal intensities of the mCherry channel were divided by the intensities of the GFP channel using the image calculator function. mCherry to sfGFP ratios were visualised by changing the grayscale values of the resulting image to false color using the ImageJ lookup table Fire. Since the ratios are sensitive to microscope settings, only ratios calculated with identical configuration of the microscope were compared. For visualisation of the nucleus, nuclear DNA was stained by leaf infiltration of 0.3 µM 4′,6-diamidino-2-phenylindole (DAPI) for 10 min. The DAPI specific fluorescence was detected at 450 nm after excitation at 405 nm with Nikon A1R confocal microscope.

Nicotiana benthamiana transfection and confocal microscopy

Growth and agroinfiltration of *Nicotiana benthamiana* were performed according to Sparkes et al. (2006) and Li (2011). Images were acquired 2 d after infiltration using a Zeiss LSM 780 confocal microscope with sfGFP excitation at 488 nm and emission at 501–522 nm, and mCherry excitation at 561 nm and emission at 600–622 nm. Within an experiment, all images were acquired using identical settings. The mCherry signal was false-coloured magenta for presentation. Scatter plots of mCherry and sfGFP intensities were acquired using the co-localisation function of ZEN 2010 imaging software (Zeiss). Co-localisation was performed on a pixel-by-pixel basis.

Immunoblotting

Protein extraction and immunoblotting were performed as in (Zhang et al., 2018). Primary antibodies were used at the following dilutions: anti-mCherry (ab183628, Abcam, Cambridge, UK), 1:3,000; anti-GFP from mouse IgG1κ (clones 7.1 and 13.1, Roche, Basel, Switzerland), 1:1,000. The secondary antibodies used were anti-rabbit horseradish peroxidase conjugate (A0545, Sigma) diluted 1:50,000 for mCherry or m-IgGκ BP-HRP (sc-516102, Santa Cruz Biotechnology, Dallas, USA) diluted 1:5,000 for GFP. Blots were then washed and developed with ECL reagent SuperSignal West Pico Chemiluminescent Substrate or SuperSignal™ West Femto Maximum Sensitivity Substrate (ThermoFisher Scientific, UK), as required.

555 *Statistical analysis*

556 Statistical analysis was routinely performed using SigmaPlot 12.5 software (Systat Inc., U.
557 S.). Different data sets were analysed for statistical significance with the One Way Repeated
558 Measures Analysis of Variance (one-way RM ANOVA), which uses the Holm-Sidak method
559 for multiple pairwise comparisons. Normality distribution of data points was tested with the
560 Shapiro-Wilk method (p to reject was $p>0.05$). Letters indicate significant difference ($p <$
561 0.05) in the figures.

562

563 **Accession numbers**

564 Sequence data from this article can be found in the GenBank data library under accession
565 numbers At5g56760 (SAT5), At3g24800 (PRT1), At5g02310 (PRT6), At1g04250 (IAA17),
566 At5g25890 (IAA28), At3g17600 (IAA31), At3g62980 (TIR1), and At3g26810 (AFB2).

567

568

569 **Supplemental Data**

570 **Supplemental Figure S1.** Nuclear-cytosolic localisation of X-tFT.

571 **Supplemental Figure S2.** Phenotype of seedlings expressing IAA-tFT fusions.

572 **Supplemental Figure S3.** Phenotype of seedlings expressing IAA31-tFT.

573 **Supplemental Figure S4.** IAA-tFT stability in Arabidopsis thaliana roots.

574 **Supplemental Figure S5.** Bortezomib stabilises IAA28-tFT and IAA31-tFT.

575 **Supplemental Figure S6.** Attributes of fluorescent reporters used in the mCherry-sfGFP
576 tandem fluorescent protein timer.

577 **Supplemental Table S1.** Primers used in this study

578

579 **Acknowledgements**

580 We thank Michael Knop for many useful discussions, and for critical reading of the
581 manuscript. We are grateful to Malcolm Bennett and Stephan Kepinski for the gift of *tir1-1*
582 *afb2* seeds, George Lund for assistance with constructs, Graham Shephard for photography,
583 Smita Kurup for useful discussions and Steve Thomas for the cDNA library.

584

585

Table 1. Literature values for Aux/IAA half-lives

NLS, nuclear localisation signal; LUC, luciferase; $t_{1/2}$, half-life

Protein/construct	Treatment	Assay	$t_{1/2}$	Ref
IAA17		^{35}S-Met labelling, cycloheximide chase and immunoprecipitation from Arabidopsis seedlings	~80 min	Ouellet et al. 2001
$IAA17_{P88L}$ (*axr3-1*)			~550 min	Ouellet et al. 2001
YFP-IAA17-NLS		Inducible expression and time-lapse flow cytometry in yeast expressing TIR1	~22 min	Moss et al., 2015
UBQ::IAA17-LUC		Cycloheximide chase and LUC imaging in Arabidopsis seedlings	11 min	Dreher et al. 2006
UBQ::$IAA17_{1-111}$-LUC-NLS			10 min	Dreher et al. 2006
UBQ::$IAA17_{1-111}$-LUC-NLS	5 µM 2,4-D		4.6 min	Dreher et al. 2006
UBQ::IAA28-LUC			~60-80 min	Dreher et al. 2006
UBQ::IAA28-LUC	5 µM 2,4-D		~15 min	Dreher et al. 2006
YFP-IAA28-NLS		Inducible expression and time-lapse flow cytometry in yeast expressing TIR1	~25 min	Moss et al., 2015
35S::IAA31-10xMyc		Cycloheximide chase and quantification with α-Myc antibody	>20 h	Dreher et al. 2006
35S::IAA31-10xMyc	10 µM 2,4-D		~4 h	Dreher et al. 2006

Figure legends

Figure 1. C-terminal mCherry-sfGFP demonstrates cytosolic localisation of SAT5

A, *Nicotiana benthamiana* leaves were transiently transformed with a construct expressing SAT5-tFT under the control of the *CaMV35S* promoter. The panels show false-coloured confocal micrographs of three different cells, counterstained with DAPI to mark nuclei. Bar: 30 µm. B, Immunoblots of different leaves infiltrated with the P19 suppressor of gene silencing (left) or SAT5-tFT plus P19 (middle and right). Blots (50 mg protein/lane) were probed with antisera towards GFP or mCherry, as indicated. The lower panels show Ponceau S staining following transfer and positions of molecular weight markers (kDa) are indicated to the left. The open arrowhead indicates the position of SAT5-tFT and the black arrowhead indicates a P19-specific band.

Figure 2. Transient expression of N-end rule tFT reporters in *Arabidopsis thaliana*

A, Generation of N-end rule tFT reporters. Constructs are driven by the constitutive *CaMV35S* promoter and encode a fusion of ubiquitin (Ub; grey) to the tandem timer (magenta and green). De-ubiquitinating enzymes remove Ub co-translationally to reveal a new N-terminus (a variable residue, indicated by X). A flexible linker (brown box) contains lysine (K) residues which can be covalently linked to ubiquitin via the sequential activity of E1, E2 and E3 enzymes. Where X is a destabilising residue (R or F), the respective E3 ligase (PRT6 or PRT1) directs the fusion protein for proteasomal degradation (modified from Kmelinskii et al., 2012). B, Quantification of relative protein stability (mCherry/sfGFP ratio) of the N-end rule tFT reporters in epidermal cells of 5-week-old wild-type plants and N-end rule E3-ligase-deficient mutants (*prt1-1* and *prt6-5*). Different letters indicate statistically significant differences between groups determined with the one-way RM ANOVA test (P<0.05, n = 4–13). Values represent means ± standard error (SE). C, Representative false-colour images of Arabidopsis leaf epidermal cells expressing N-end rule-tFT reporters for calculation of mCherry/sfGFP ratios (blue = unstable; white = stable. The heat map indicates the intensity ratio of mCherry to sfGFP. Bar: 20 µm.

Figure 3. Stable expression of N-end rule tFT reporters in *Arabidopsis thaliana*

A and B, Immunoblots of transgenic lines expressing R-tFT (A) and F-tFT (B). Two independent transgenic lines were selected for each construct and crossed to Col-0 to obtain a control line harbouring the same transgene event. Proteins were extracted from 5-d-old seedlings treated with 50 µM Bortezomib or DMSO and subjected to immunoblotting (20 µg/lane) with antisera towards GFP or mCherry. The lower panels show Ponceau S staining following transfer and positions of molecular weight markers (kDa) are indicated to the left. C, Quantification of relative protein stability (mCherry/sfGFP ratio) of the N-end rule tFT reporters in root cells of 7-d-old wild-type plants and N-end rule E3-ligase-deficient mutants (*prt1-1* and *prt6-5*) treated for 4 h with the proteasome inhibitor MG-132 (50 µM). Different letters indicate statistically significant differences between groups determined with the one-way RM ANOVA test (P<0.05, n = 4-7). Values represent means ± standard error (SE). D, Representative false-colour images of Arabidopsis root cells expressing N-end rule-tFT reporters for calculation of mCherry/sfGFP ratios (blue = unstable; while = stable). The heat map indicates the intensity ratio of mCherry to sfGFP. Bar: 20 µm.

Figure 4. Transient expression of IAA-tFT reporters in *N. benthamiana* epidermis

A-D, Representative confocal micrographs of *N. benthamiana* leaf epidermal cells agroinfiltrated with different IAA-tFT constructs. Panels clockwise from top left: sfGFP, mCherry, merge, bright field. Bar = 50 µm. B, Plots showing relative intensity of mCherry and

sfGFP signals on a pixel-by-pixel basis. The colour in the plot represents the number of pixels (absolute frequency) that are plotted in that region.

Figure 5. Transient expression of IAA-tFT reporters in *Arabidopsis thaliana*

A, Quantification of relative protein stability (mCherry/sfGFP ratio) of IAA-tFT reporters in epidermal cells of 5-week-old wild-type plants treated for 2 h with 100 µM 2,4-D or ethanol (EtOH, n = 4-7). Values represent means ± standard error (SE). B, Representative false-colour images of Arabidopsis epidermal cells expressing IAA-tFT reporters for calculation of mCherry/sfGFP rations shown in A (blue = unstable; white = stable). The heat map indicates the intensity ratio of mCherry to sfGFP. Nuclear (nuc) and cytosolic (cyt) data were collected separately for IAA17. As a result of significant destabilisation of the cytosolic IAA17-tFT by 2,4-D treatment, the mCherry signal was undetectable. In this case, the signals for sfGFP and mCherry of the IAA17-tFT were shown in separate images (red frame). Bar: 15 µm. C, mCherry/sfGFP ratios of IAA28-tFT transiently transformed in wild type and the *tir1-1 afb2* double mutant lacking the auxin-activated degradation system (n=8). D, Representative false-colour images of Arabidopsis epidermal cells expressing IAA-tFT reporters for calculation of mCherry/sfGFP rations shown in C (blue = unstable; white = stable bar: 15 µm. The heat map indicates the intensity ratio of mCherry to sfGFP. Different letters indicate statistically significant differences between groups determined with the one-way RM ANOVA test (P<0.05). Values represent means ± standard error (SE).

Figure 6. Stable expression of IAA-tFT reporters in *Arabidopsis thaliana*

Immunoblots of stable Arabidopsis transgenic lines expressing different IAA genes fused to tFT. Five-d-old seedlings were treated with 5 µM 2,4-D or ethanol (EtOH) for 4 h. Blots (40 µg/lane) were probed with anti-GFP or anti-mCherry antibodies (black arrowheads indicate a non-specific band recognised by the mCherry antibody; white arrowheads indicate the IAA-tFT proteins). The lower panels show Ponceau S staining following transfer and positions of molecular weight markers (kDa) are indicated to the left.

Figure 7. Auxin destabilises IAA31-tFT *in planta*

A, Confocal micrographs of primary roots of 6-d-old IAA31-tFT seedlings, treated with 5 µM 2,4-D or ethanol (cont.) for 4 h. B, Confocal micrographs of 14-d-old IAA31-tFT roots turned by 180° for 16 h to induce root bending. Bar: 50 µm.

Literature Cited

Abel S, Oeller PW, Theologis A (1994) Early auxin-induced genes encode short-lived nuclear proteins. Proc Natl Acad Sci U S A **91:** 326-330

Alber AB, Paquet ER, Biserni M, Naef F, Suter DM (2018) Single Live Cell Monitoring of Protein Turnover Reveals Intercellular Variability and Cell-Cycle Dependence of Degradation Rates. Mol Cell **71:** 1079-1091 e1079

Arase F, Nishitani H, Egusa M, Nishimoto N, Sakurai S, Sakamoto N, Kaminaka H (2012) IAA8 involved in lateral root formation interacts with the TIR1 auxin receptor and ARF transcription factors in Arabidopsis. PLoS One **7:** e43414

Bachmair A, Finley D, Varshavsky A (1986) In vivo half-life of a protein is a function of its amino-terminal residue. Science **234:** 179-186

Barry JD, Dona E, Gilmour D, Huber W (2016) TimerQuant: a modelling approach to tandem fluorescent timer design and data interpretation for measuring protein turnover in embryos. Development **143:** 174-179

Bensimon A, Heck AJ, Aebersold R (2012) Mass spectrometry-based proteomics and network biology. Annu Rev Biochem **81:** 379-405

Boisvert FM, Ahmad Y, Gierlinski M, Charriere F, Lamont D, Scott M, Barton G, Lamond AI (2012) A quantitative spatial proteomics analysis of proteome turnover in human cells. Mol Cell Proteomics **11:** M111 011429

Brunoud G, Wells DM, Oliva M, Larrieu A, Mirabet V, Burrow AH, Beeckman T, Kepinski S, Traas J, Bennett MJ, Vernoux T (2012) A novel sensor to map auxin response and distribution at high spatio-temporal resolution. Nature **482:** 103-106

Calderón Villalobos LI, Lee S, De Oliveira C, Ivetac A, Brandt W, Armitage L, Sheard LB, Tan X, Parry G, Mao H, Zheng N, Napier R, Kepinski S, Estelle M (2012) A combinatorial TIR1/AFB-Aux/IAA co-receptor system for differential sensing of auxin. Nat Chem Biol **8:** 477-485

Ciechanover A (2013) Intracellular protein degradation: from a vague idea through the lysosome and the ubiquitin-proteasome system and onto human diseases and drug targeting. Bioorg Med Chem **21:** 3400-3410

Claydon AJ, Beynon R (2012) Proteome dynamics: revisiting turnover with a global perspective. Mol Cell Proteomics **11:** 1551-1565

De Rybel B, Vassileva V, Parizot B, Demeulenaere M, Grunewald W, Audenaert D, Van Campenhout J, Overvoorde P, Jansen L, Vanneste S, Möller B, Wilson M, Holman T, Van Isterdael G, Brunoud G, Vuylsteke M, Vernoux T, De Veylder L, Inzé D, Weijers D, Bennett MJ, Beeckman T (2010) A Novel Aux/IAA28 Signaling Cascade Activates GATA23-Dependent Specification of Lateral Root Founder Cell Identity. Current Biology **20:** 1697-1706

Dharmasiri N, Dharmasiri S, Estelle M (2005a) The F-box protein TIR1 is an auxin receptor. Nature **435:** 441-445

Dharmasiri N, Dharmasiri S, Weijers D, Lechner E, Yamada M, Hobbie L, Ehrismann JS, Jurgens G, Estelle M (2005b) Plant development is regulated by a family of auxin receptor F box proteins. Dev Cell **9:** 109-119

Doherty MK, Hammond DE, Clague MJ, Gaskell SJ, Beynon RJ (2009) Turnover of the human proteome: determination of protein intracellular stability by dynamic SILAC. J Proteome Res **8:** 104-112

Dona E, Barry JD, Valentin G, Quirin C, Khmelinskii A, Kunze A, Durdu S, Newton LR, Fernandez-Minan A, Huber W, Knop M, Gilmour D (2013) Directional tissue migration through a self-generated chemokine gradient. Nature **503:** 285-289

Dreher KA, Brown J, Saw RE, Callis J (2006) The Arabidopsis Aux/IAA protein family has diversified in degradation and auxin responsiveness. Plant Cell **18:** 699-714

Durrieu L, Kirrmaier D, Schneidt T, Kats I, Raghavan S, Hufnagel L, Saunders TE, Knop M (2018) Bicoid gradient formation mechanism and dynamics revealed by protein lifetime analysis. Molecular systems biology **14:** e8355-e8355

Eden E, Geva-Zatorsky N, Issaeva I, Cohen A, Dekel E, Danon T, Cohen L, Mayo A, Alon U (2011) Proteome half-life dynamics in living human cells. Science **331:** 764-768

Friml J (2010) Subcellular trafficking of PIN auxin efflux carriers in auxin transport. Eur J Cell Biol **89:** 231-235

Gallagher KL, Sozzani R, Lee CM (2014) Intercellular protein movement: deciphering the language of development. Annu Rev Cell Dev Biol **30:** 207-233

Garzón M, Eifler K, Faust A, Scheel H, Hofmann K, Koncz C, Yephremov A, Bachmair A (2007) PRT6/At5g02310 encodes an Arabidopsis ubiquitin ligase of the N-end rule pathway with arginine specificity and is not the CER3 locus. FEBS Lett **581:** 3189-3196

Gibbs DJ, Bacardit J, Bachmair A, Holdsworth MJ (2014) The eukaryotic N-end rule pathway: conserved mechanisms and diverse functions. Trends Cell Biol **24:** 603-611

Gibbs DJ, Bailey M, Tedds HM, Holdsworth MJ (2016) From start to finish: amino-terminal protein modifications as degradation signals in plants. New Phytol **211:** 1188-1194

Gibbs DJ, Lee SC, Isa NM, Gramuglia S, Fukao T, Bassel GW, Correia CS, Corbineau F, Theodoulou FL, Bailey-Serres J, Holdsworth MJ (2011) Homeostatic response to hypoxia is regulated by the N-end rule pathway in plants. Nature **479:** 415-418

Graciet E, Walter F, Maoileidigh DO, Pollmann S, Meyerowitz EM, Varshavsky A, Wellmer F (2009) The N-end rule pathway controls multiple functions during Arabidopsis shoot and leaf development. Proc Natl Acad Sci U S A **106:** 13618-13623

Gray WM, Kepinski S, Rouse D, Leyser O, Estelle M (2001) Auxin regulates SCF(TIR1)-dependent degradation of AUX/IAA proteins. Nature **414:** 271-276

Gross LA, Baird GS, Hoffman RC, Baldridge KK, Tsien RY (2000) The structure of the chromophore within DsRed, a red fluorescent protein from coral. PNAS **97:** 11990-11995

Habets ME, Offringa R (2014) PIN-driven polar auxin transport in plant developmental plasticity: a key target for environmental and endogenous signals. New Phytol **203:** 362-377

Holman SW, Hammond DE, Simpson DM, Waters J, Hurst JL, Beynon RJ (2016) Protein turnover measurement using selected reaction monitoring-mass spectrometry (SRM-MS). Philos Trans A Math Phys Eng Sci **374**

Hua Z, Vierstra RD (2011) The cullin-RING ubiquitin-protein ligases. Annu Rev Plant Biol **62:** 299-334

Hwang CS, Shemorry A, Varshavsky A (2010) N-terminal acetylation of cellular proteins creates specific degradation signals. Science **327:** 973-977
Karimi M, Bleys A, Vanderhaeghen R, Hilson P (2007) Building blocks for plant gene assembly. Plant Physiol **145:** 1183-1191
Karimi M, De Meyer B, Hilson P (2005) Modular cloning in plant cells. Trends Plant Sci **10:** 103-105
Kats I, Khmelinskii A, Kschonsak M, Huber F, Kniess RA, Bartosik A, Knop M (2018) Mapping Degradation Signals and Pathways in a Eukaryotic N-terminome. Mol Cell **70:** 488-501 e485
Kepinski S, Leyser O (2005) The Arabidopsis F-box protein TIR1 is an auxin receptor. Nature **435:** 446-451
Khmelinskii A, Keller PJ, Bartosik A, Meurer M, Barry JD, Mardin BR, Kaufmann A, Trautmann S, Wachsmuth M, Pereira G, Huber W, Schiebel E, Knop M (2012) Tandem fluorescent protein timers for in vivo analysis of protein dynamics. Nat Biotechnol **30:** 708-714
Khmelinskii A, Knop M (2014) Analysis of protein dynamics with tandem fluorescent protein timers. Methods Mol Biol **1174:** 195-210
Khmelinskii A, Meurer M, Ho CT, Besenbeck B, Fuller J, Lemberg MK, Bukau B, Mogk A, Knop M (2016) Incomplete proteasomal degradation of green fluorescent proteins in the context of tandem fluorescent protein timers. Mol Biol Cell **27:** 360-370
Knop M, Edgar BA (2014) Tracking protein turnover and degradation by microscopy: photo-switchable versus time-encoded fluorescent proteins. Open Biol **4:** 140002
Kraut DA, Israeli E, Schrader EK, Patil A, Nakai K, Nanavati D, Inobe T, Matouschek A (2012) Sequence- and species-dependence of proteasomal processivity. ACS Chem Biol **7:** 1444-1453
Kumar S, de Boer R, van der Klei IJ (2018) Yeast cells contain a heterogeneous population of peroxisomes that segregate asymmetrically during cell division. J Cell Sci **131**
Larrieu AP, French AP, Pridmore TP, Bennett MJ, Wells DM (2014) Time-profiling fluorescent reporters in the Arabidopsis root. Methods Mol Biol **1056:** 11-17
Laskowski M, Grieneisen VA, Hofhuis H, Hove CA, Hogeweg P, Maree AF, Scheres B (2008) Root system architecture from coupling cell shape to auxin transport. PLoS Biol **6:** e307
Lee JY, Colinas J, Wang JY, Mace D, Ohler U, Benfey PN (2006) Transcriptional and posttranscriptional regulation of transcription factor expression in Arabidopsis roots. Proc Natl Acad Sci U S A **103:** 6055-6060
Leyser HM, Pickett FB, Dharmasiri S, Estelle M (1996) Mutations in the AXR3 gene of Arabidopsis result in altered auxin response including ectopic expression from the SAUR-AC1 promoter. Plant J **10:** 403-413
Li L, Nelson CJ, Trosch J, Castleden I, Huang S, Millar AH (2017) Protein Degradation Rate in Arabidopsis thaliana Leaf Growth and Development. Plant Cell **29:** 207-228
Li X (2011) Infiltration of Nicotiana benthamiana Protocol for Transient Expression via Agrobacterium. Bio-protocol **1:** e95
Licausi F, Kosmacz M, Weits DA, Giuntoli B, Giorgi FM, Voesenek LA, Perata P, van Dongen JT (2011) Oxygen sensing in plants is mediated by an N-end rule pathway for protein destabilization. Nature **479:** 419-422
Linster E, Stephan I, Bienvenut WV, Maple-Grodem J, Myklebust LM, Huber M, Reichelt M, Sticht C, Geir Moller S, Meinnel T, Arnesen T, Giglione C, Hell

R, Wirtz M (2015) Downregulation of N-terminal acetylation triggers ABA-mediated drought responses in Arabidopsis. Nat Commun **6:** 7640

Linster E, Wirtz M (2018) N-terminal acetylation: an essential protein modification emerges as an important regulator of stress responses. J Exp Bot **69:** 4555-4568

Long Y, Scheres B, Blilou I (2015) The logic of communication: roles for mobile transcription factors in plants. J Exp Bot **66:** 1133-1144

Mangano S, Gonzalez CD, Petruccelli S (2014) Agrobacterium tumefaciens-mediated transient transformation of Arabidopsis thaliana leaves. Methods Mol Biol **1062:** 165-173

Miricescu A, Goslin K, Graciet E (2018) Ubiquitylation in plants: signaling hub for the integration of environmental signals. J Exp Bot **69:** 4511-4527

Moss BL, Mao H, Guseman JM, Hinds TR, Hellmuth A, Kovenock M, Noorassa A, Lanctot A, Villalobos LI, Zheng N, Nemhauser JL (2015) Rate Motifs Tune Auxin/Indole-3-Acetic Acid Degradation Dynamics. Plant Physiol **169:** 803-813

Mot AC, Prell E, Klecker M, Naumann C, Faden F, Westermann B, Dissmeyer N (2018) Real-time detection of N-end rule-mediated ubiquitination via fluorescently labeled substrate probes. New Phytol **217:** 613-624

Nelson CJ, Li L, Jacoby RP, Millar AH (2013) Degradation rate of mitochondrial proteins in *Arabidopsis thaliana* cells. J Proteome Res **12:** 3449-3459

Nelson CJ, Li L, Millar AH (2014) Quantitative analysis of protein turnover in plants. Proteomics **14:** 579-592

Nelson CJ, Millar AH (2015) Protein turnover in plant biology. Nature Plants **1:** 15017

Ottenschläger I, Wolff P, Wolverton C, Bhalerao RP, Sandberg G, Ishikawa H, Evans M, Palme K (2003) Gravity-regulated differential auxin transport from columella to lateral root cap cells. Proc Natl Acad Sci U S A **100:** 2987-2991

Ouellet F, Overvoorde PJ, Theologis A (2001) IAA17/AXR3: Biochemical Insight into an Auxin Mutant Phenotype. Plant Cell **13:** 829-841

Podolec R, Ulm R (2018) Photoreceptor-mediated regulation of the COP1/SPA E3 ubiquitin ligase. Curr Opin Plant Biol **45:** 18-25

Potuschak T, Stary S, Schlogelhofer P, Becker F, Nejinskaia V, Bachmair A (1998) PRT1 of Arabidopsis thaliana encodes a component of the plant N-end rule pathway. Proc Natl Acad Sci U S A **95:** 7904-7908

Ramos JA, Zenser N, Leyser O, Callis J (2001) Rapid degradation of auxin/indoleacetic acid proteins requires conserved amino acids of domain II and is proteasome dependent. Plant Cell **13:** 2349-2360

Reed JW (2001) Roles and activities of Aux/IAA proteins in Arabidopsis. Trends Plant Sci **6:** 420-425

Rogg LE, Lasswell J, Bartel B (2001) A gain-of-function mutation in IAA28 suppresses lateral root development. Plant Cell **13:** 465-480

Rouse D, Mackay P, Stirnberg P, Estelle M, Leyser O (1998) Changes in auxin response from mutations in an AUX/IAA gene. Science **279:** 1371-1373

Sato A, Yamamoto KT (2008) Overexpression of the non-canonical Aux/IAA genes causes auxin-related aberrant phenotypes in Arabidopsis. Physiol Plant **133:** 397-405

Sato EM, Hijazi H, Bennett MJ, Vissenberg K, Swarup R (2015) New insights into root gravitropic signalling. J Exp Bot **66:** 2155-2165

Savitski MM, Zinn N, Faelth-Savitski M, Poeckel D, Gade S, Becher I, Muelbaier M, Wagner AJ, Strohmer K, Werner T, Melchert S, Petretich M,

Rutkowska A, Vappiani J, Franken H, Steidel M, Sweetman GM, Gilan O, Lam EYN, Dawson MA, Prinjha RK, Grandi P, Bergamini G, Bantscheff M (2018) Multiplexed Proteome Dynamics Profiling Reveals Mechanisms Controlling Protein Homeostasis. Cell **173:** 260-274.e225

Schwanhäusser B, Busse D, Li N, Dittmar G, Schuchhardt J, Wolf J, Chen W, Selbach M (2011) Global quantification of mammalian gene expression control. Nature **473:** 337-342

Seibel NM, Eljouni J, Nalaskowski MM, Hampe W (2007) Nuclear localization of enhanced green fluorescent protein homomultimers. Anal Biochem **368:** 95-99

Shemiakina, II, Ermakova GV, Cranfill PJ, Baird MA, Evans RA, Souslova EA, Staroverov DB, Gorokhovatsky AY, Putintseva EV, Gorodnicheva TV, Chepurnykh TV, Strukova L, Lukyanov S, Zaraisky AG, Davidson MW, Chudakov DM, Shcherbo D (2012) A monomeric red fluorescent protein with low cytotoxicity. Nat Commun **3:** 1204

Sparkes IA, Runions J, Kearns A, Hawes C (2006) Rapid, transient expression of fluorescent fusion proteins in tobacco plants and generation of stably transformed plants. Nat Protoc **1:** 2019-2025

Stary S, Yin XJ, Potuschak T, Schlogelhofer P, Nizhynska V, Bachmair A (2003) PRT1 of Arabidopsis is a ubiquitin protein ligase of the plant N-end rule pathway with specificity for aromatic amino-terminal residues. Plant Physiol **133:** 1360-1366

Swarup R, Kramer EM, Perry P, Knox K, Leyser HM, Haseloff J, Beemster GT, Bhalerao R, Bennett MJ (2005) Root gravitropism requires lateral root cap and epidermal cells for transport and response to a mobile auxin signal. Nat Cell Biol **7:** 1057-1065

Tao LZ, Cheung AY, Nibau C, Wu HM (2005) RAC GTPases in tobacco and Arabidopsis mediate auxin-induced formation of proteolytically active nuclear protein bodies that contain AUX/IAA proteins. Plant Cell **17:** 2369-2383

Tian Q, Reed JW (1999) Control of auxin-regulated root development by the Arabidopsis thaliana SHY2/IAA3 gene. Development **126:** 711-721

Varshavsky A (2000) Ubiquitin fusion technique and its descendants. Methods Enzymol **327:** 578-593

Varshavsky A (2011) The N-end rule pathway and regulation by proteolysis. Protein Sci **20:** 1298-1345

Vicente J, Mendiondo GM, Movahedi M, Peirats-Llobet M, Juan Y-t, Shen Y-y, Dambire C, Smart K, Rodriguez PL, Charng Y-y, Gray JE, Holdsworth MJ (2017) The Cys-Arg/N-End Rule Pathway Is a General Sensor of Abiotic Stress in Flowering Plants. Current Biology **27:** 3183-3190.e3184

Vierstra RD (2009) The ubiquitin-26S proteasome system at the nexus of plant biology. Nat Rev Mol Cell Biol **10:** 385-397

Welle KA, Zhang T, Hryhorenko JR, Shen S, Qu J, Ghaemmaghami S (2016) Time-resolved Analysis of Proteome Dynamics by Tandem Mass Tags and Stable Isotope Labeling in Cell Culture (TMT-SILAC) Hyperplexing. Mol Cell Proteomics **15:** 3551-3563

Wirtz M, Birke H, Heeg C, Mueller C, Hosp F, Throm C, Koenig S, Feldman-Salit A, Rippe K, Petersen G, Wade RC, Rybin V, Scheffzek K, Hell R (2010) Structure and function of the hetero-oligomeric cysteine synthase complex in plants. J Biol Chem **285:** 32810-32817

Worley CK, Zenser N, Ramos J, Rouse D, Leyser O, Theologis A, Callis J (2000) Degradation of Aux/IAA proteins is essential for normal auxin signalling. Plant J **21:** 553-562

Xu F, Huang Y, Li L, Gannon P, Linster E, Huber M, Kapos P, Bienvenut W, Polevoda B, Meinnel T, Hell R, Giglione C, Zhang Y, Wirtz M, Chen S, Li X (2015) Two N-terminal acetyltransferases antagonistically regulate the stability of a nod-like receptor in Arabidopsis. Plant Cell **27:** 1547-1562

Zanetti ME, Chang IF, Gong F, Galbraith DW, Bailey-Serres J (2005) Immunopurification of polyribosomal complexes of Arabidopsis for global analysis of gene expression. Plant Physiol **138:** 624-635

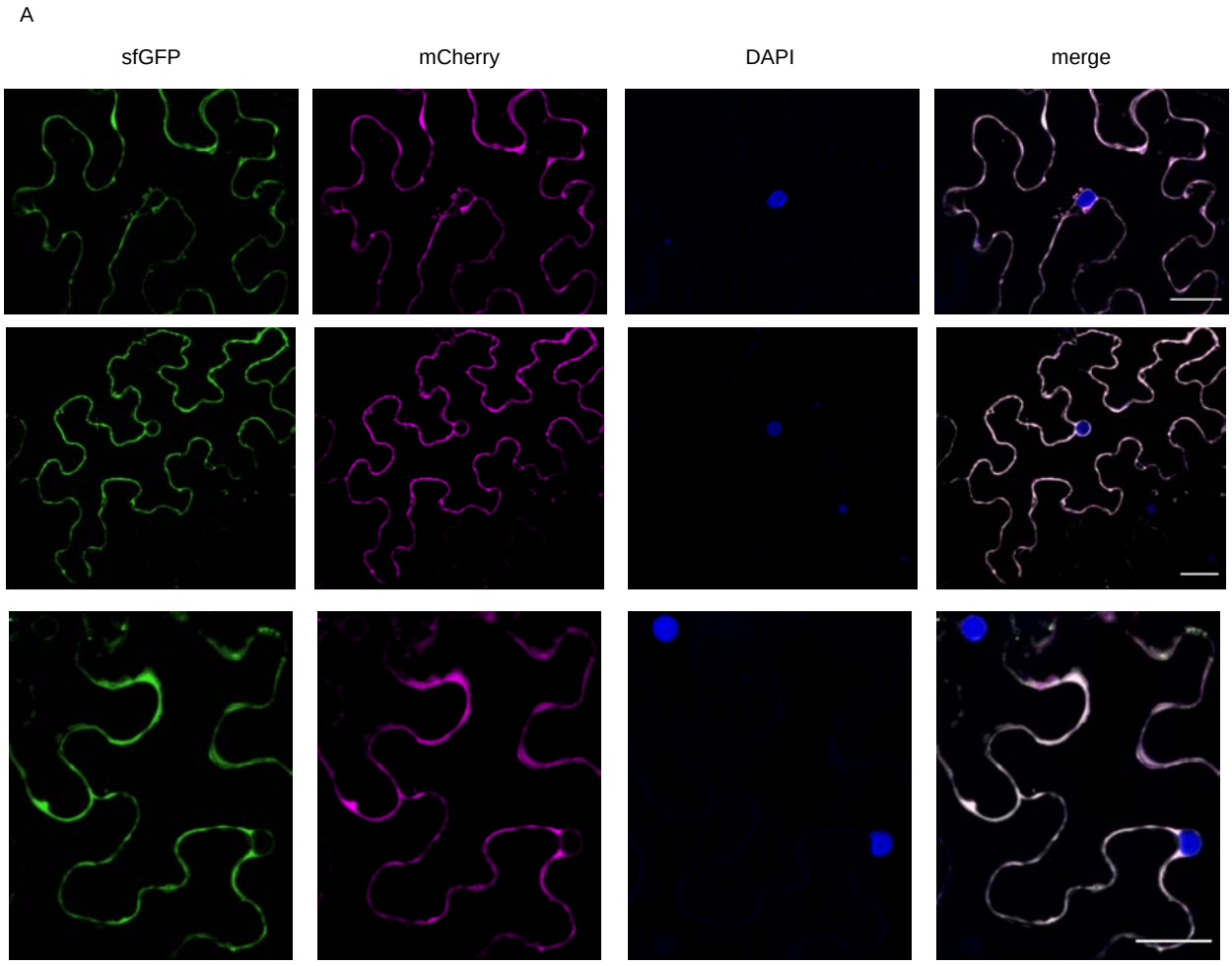

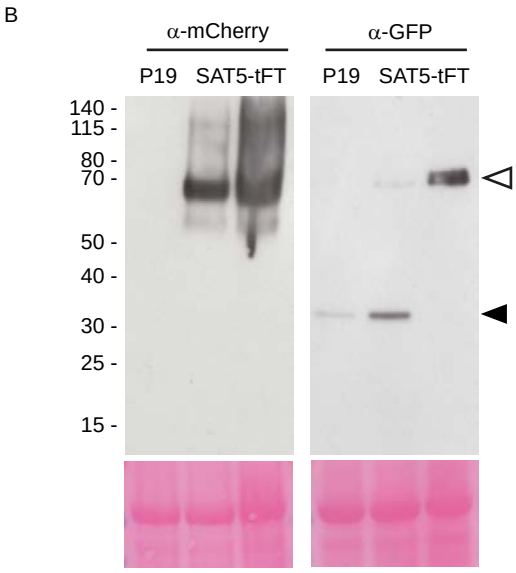

Figure 1. C-terminal mCherry-sfGFP demonstrates cytosolic localisation of SAT5
A, *Nicotiana benthamiana* leaves were transiently transformed with a construct expressing SAT5-tFT under the control of the *CaMV35S p*romoter. The panels show confocal micrographs of three different cells, counterstained with DAPI to mark nuclei. Bar: 30 μm B, Immunoblots of different leaves infiltrated with the P19 suppressor of gene silencing (left) or SAT5-tFT plus P19 (middle and right). Blots (50 μg protein/lane) were probed with antisera towards GFP or mCherry, as indicated. The lower panels show Ponceau S staining following transfer and positions of molecular weight markers (kDa) are indicated to the left.
The open arrowhead indicates the position of SAT5-tFT and the black arrowhead indicates a P19-specific band.

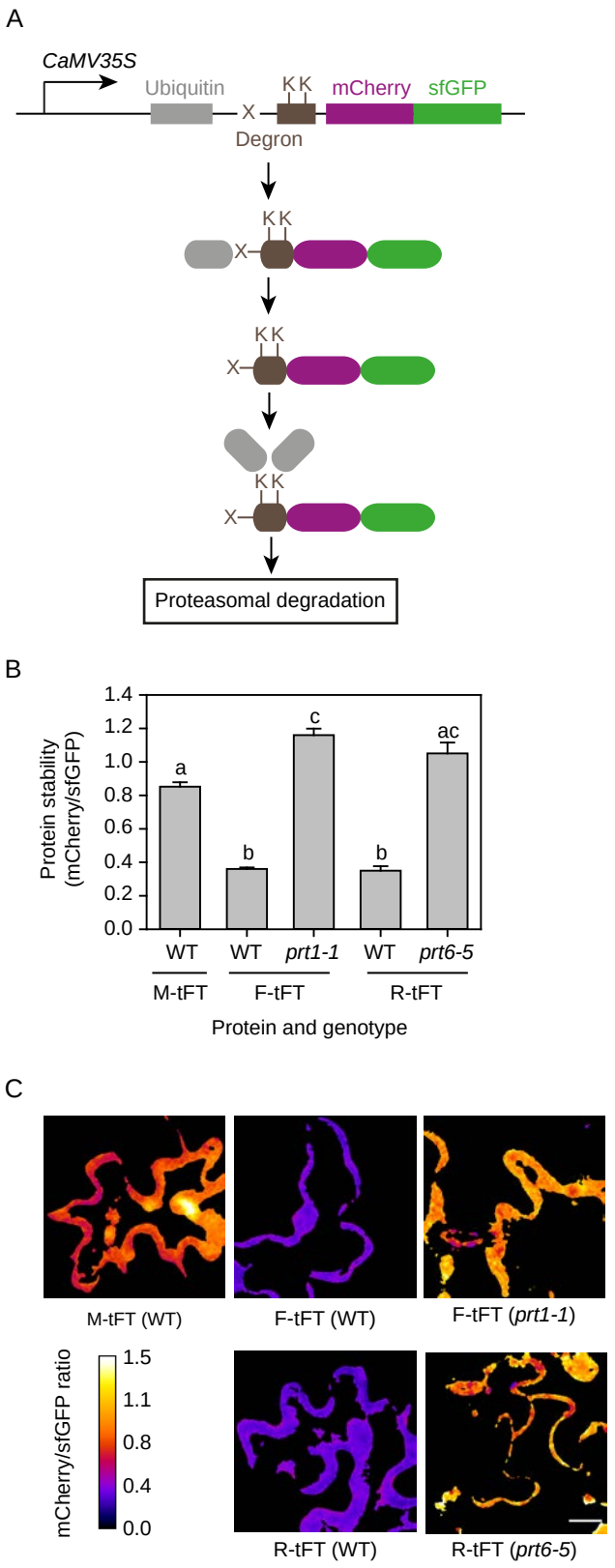

Figure 2. Transient expression of N-end rule tFT reporters in *Arabidopsis thaliana*
A, Generation of N-end rule tFT reporters. Constructs are driven by the constitutive CaMV35S promoter and encode a fusion of ubiquitin (Ub; grey) to the tandem timer (magenta and green). De-ubiquitinating enzymes remove Ub co-translationally to reveal a new N-terminus (a variable residue, indicated by X). A flexible linker (brown box) contains lysine (K) residues which can be covalently linked to ubiquitin via the sequential activity of E1, E2 and E3 enzymes. Where X is a destabilising residue (R or F), the respective E3 ligase (PRT6 or PRT1) directs the fusion protein for proteasomal degradation (modified from Kmelinskii et al., 2012). B, Quantification of relative protein stability (mCherry/sfGFP ratio) of the N-end rule tFT reporters in epidermal cells of 5-week old wild-type plants and N-end rule E3-ligase-deficient mutants (*prt1-1* and *prt6-5*). Different letters indicate statistically significant differences between groups determined with the one-way RM ANOVA test (P<0.05, n = 4-13). Values represent means +/- standard error (SE). C, Representative false-colour images of Arabidopsis leaf epidermal cells expressing N-end rule-tFT reporters for calculation of mCherry/sfGFP ratios (blue = unstable, white = stable). The heat map indicates the intensity ratio of mCherry to sfGFP. Bar: 20 μm in all panels.

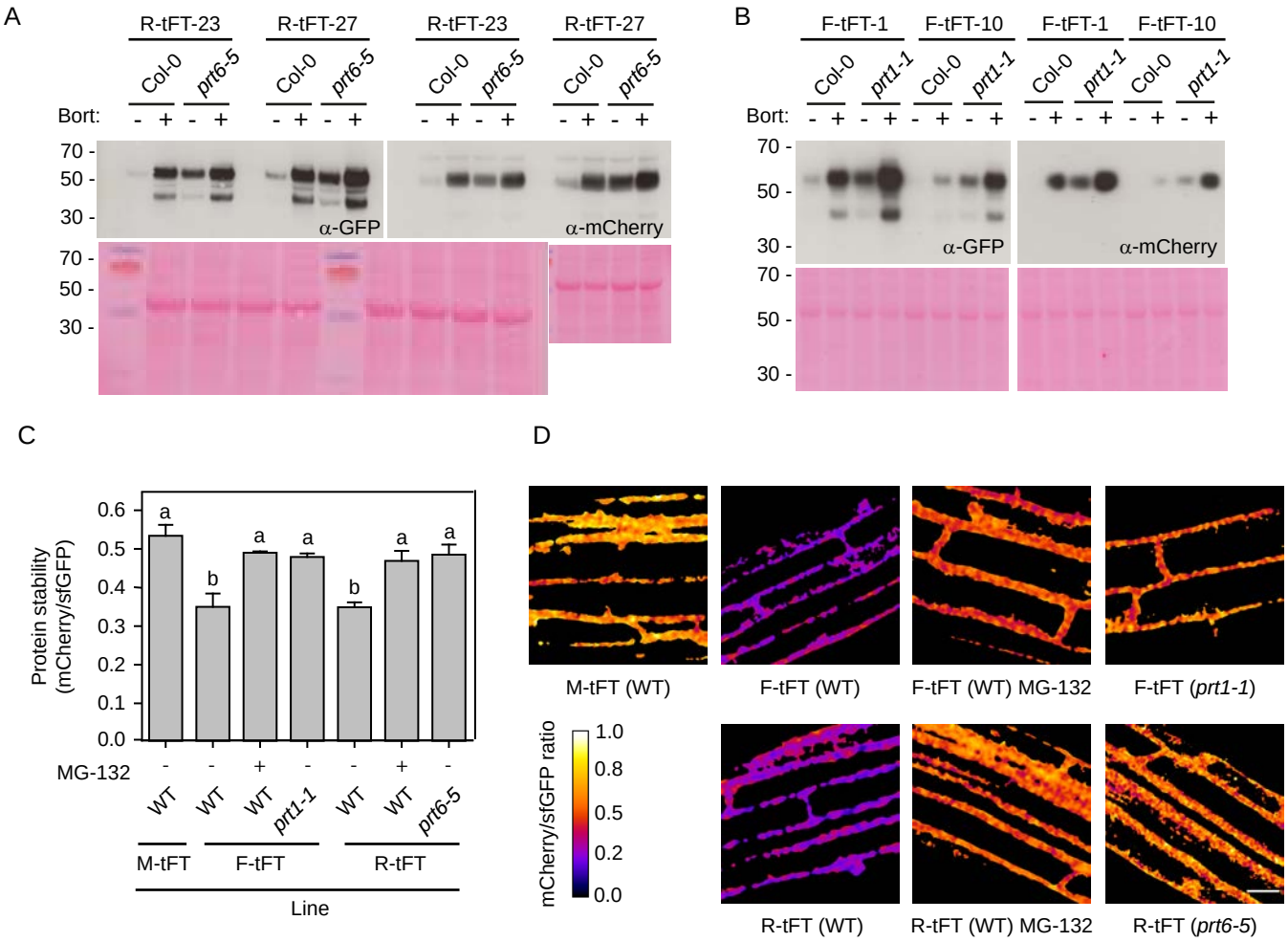

Figure 3 Stable expression of N-end rule tFT reporters in *Arabidopsis thaliana*
A, and B, Immunoblots of transgenic lines expressing R-tFT (A) and F-tFT (B). Two independent transgenic lines were selected for each construct and crossed to Col-0 to obtain a control line harbouring the same transgene event. Proteins were extracted from 5 d old seedlings treated with 50 μM Bortezomib or DMSO and subjected to immunoblotting (20 μg/lane) with antisera towards GFP or mCherry. The lower panels show Ponceau S staining following transfer and positions of molecular weight markers (kDa) are indicated to the left. C, Quantification of relative protein stability (mCherry/sfGFP ratio) of the N-end rule tFT reporters in root cells of 7 d-old wild-type plants and N-end rule E3-ligase-deficient mutants (*prt1-1* and *prt6-5*) treated for 4 h with the proteasome inhibitor MG-132 (50 μM). Different letters indicate statistically significant differences between groups determined with the one-way RM ANOVA test ($P<0.05$, n = 4-7). Values represent means + standard error (SE). D, Representative false-colour images of Arabidopsis root cells expressing N-end rule-tFT reporters for calculation of mCherry/sfGFP ratios (blue = unstable, white = stable). The heat map indicates the intensity ratio of mCherry to sfGFP Bar: 20 μm for all panels.

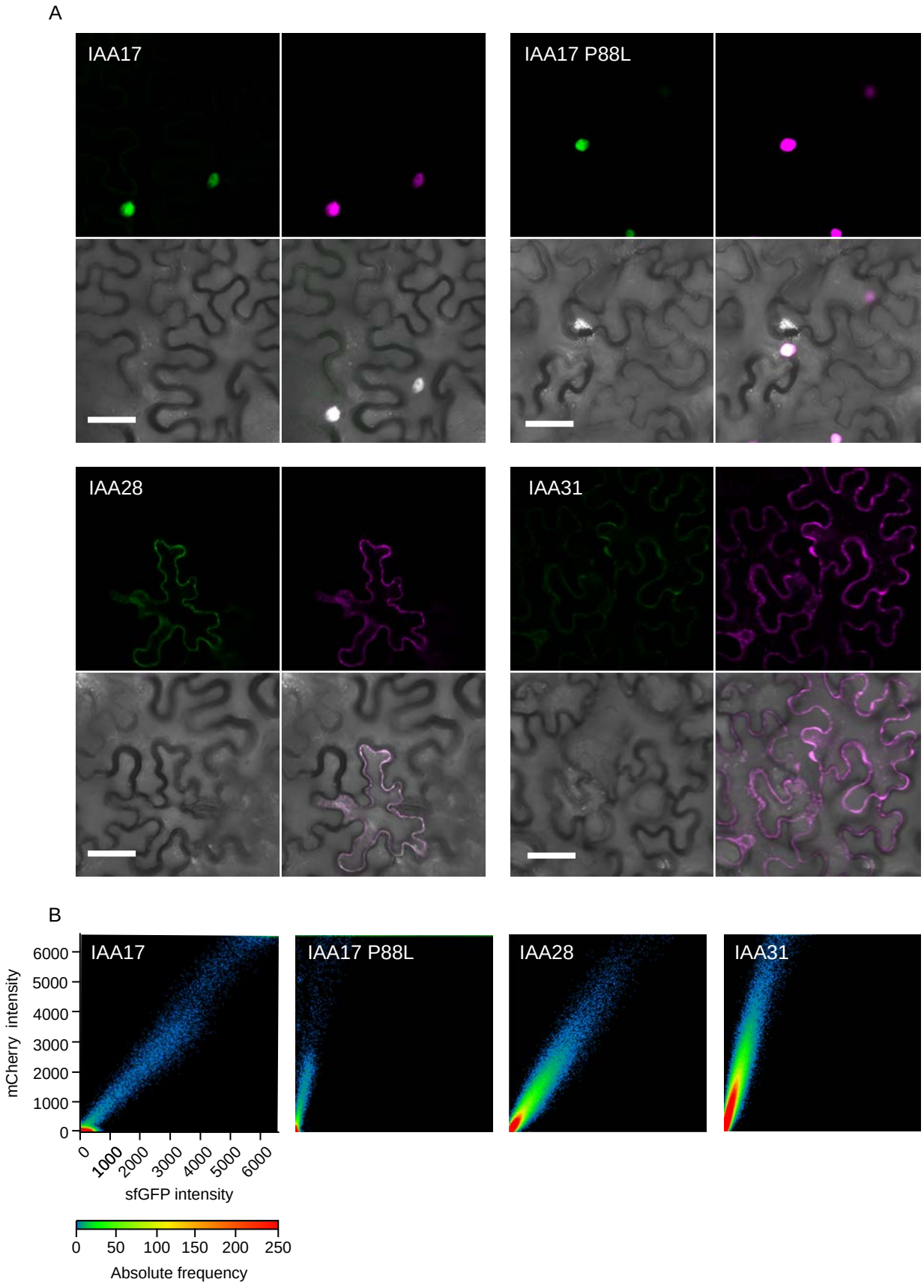

Figure 4. Transient expression of IAA-tFT reporters in *N. benthamiana* epidermis
A, Representative confocal micrographs of *N. benthamiana* leaf epidermal cells agroinfiltrated with different IAA-tFT constructs. Panels clockwise from top left: sfGFP, mCherry, merge, bright field. Bar = 50 μm. B, Plots showing relative intensity of mCherry and sfGFP signals on a pixel-by-pixel basis. The colours in the plot represent the number of pixels (absolute frequency) that are plotted in that region).

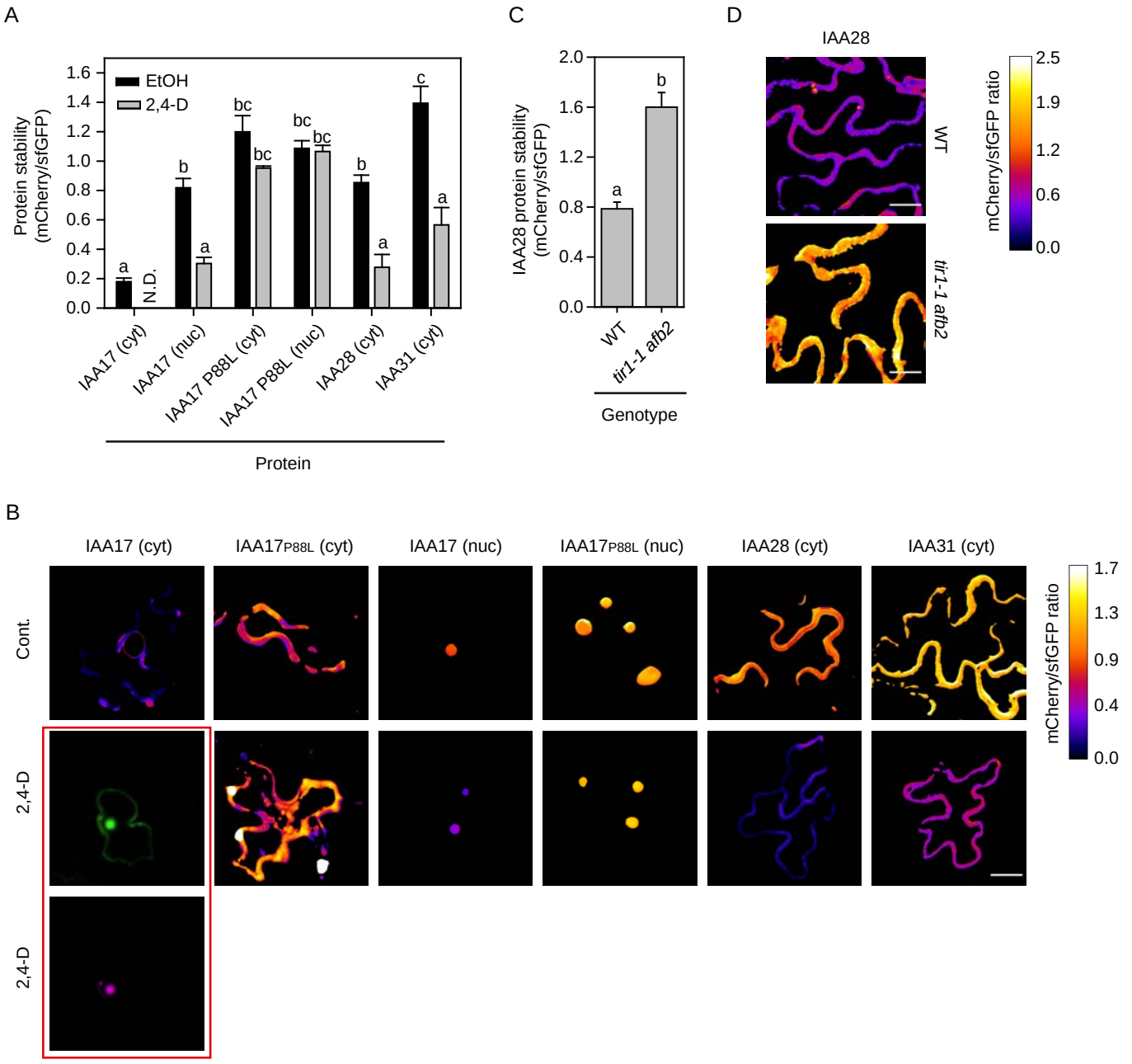

Figure 5. Transient expression of IAA-tFT reporters in *Arabidopsis thaliana*
A, Quantification of relative protein stability (mCherry/sfGFP ratio) of IAA-tFT reporters in epidermal cells of 5 week old wild-type plants treated for 2 h with 100 μM 2,4-D or ethanol (EtOH, n = 4-7). Values represent means +/- standard error (SE). B, Representative false-colour images of Arabidopsis epidermal cells expressing IAA-tFT reporters for calculation of mCherry/sfGFP ratios shown in A (blue = unstable, white = stable). The heat map indicates the intensity ratio of mCherry to sfGFP. Nuclear (nuc) and cytosolic (cyt) data were collected separately for IAA17. As a result of significant destabilisation of the cytosolic IAA17-tFT by 2,4-D treatment, the mCherry signal was undetectable. In this case, the signals for sfGFP and mCherry of the IAA17-tFT were shown in separate images (red frame). Bar: 15 μm for all panels. C, mCherry/sfGFP ratios of IAA28-tFT transiently transformed in wild type and the *tir1-1 afb2* double mutant lacking the auxin-activated degradation system (n=8). D, Representative false-colour images of Arabidopsis epidermal cells expressing IAA-tFT reporters for calculation of mCherry/sfGFP ratios shown in C (blue = unstable, white = stable); bar: 15 μm. The heat map indicates the intensity ratio of mCherry to sfGFP. Different letters indicate statistically significant differences between groups determined with the one-way RM ANOVA test (P<0.05). Values represent means +/- standard error (SE).

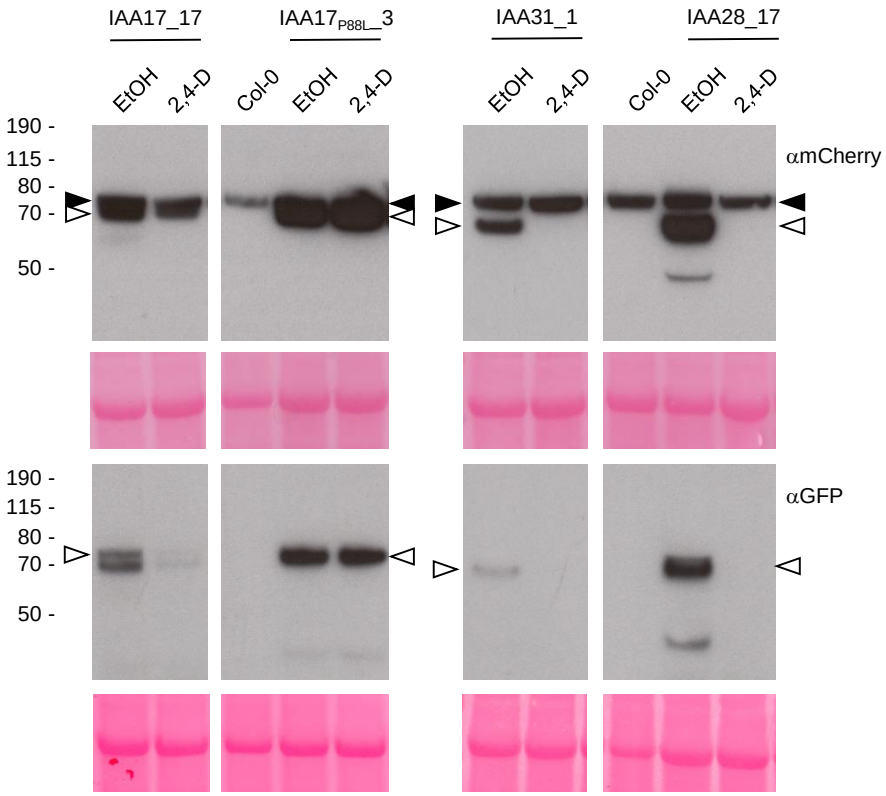

Figure 6 Stable expression of IAA-tFT reporters in *Arabidopsis thaliana*
Immunoblots of stable Arabidopsis transgenic lines expressing different IAA genes fused to tFT. Five d old seedlings were treated with 5 mM 2,4-D or ethanol (EtOH) for 4 h. Blots (40 μg/lane) were probed with anti-GFP or anti-mCherry antibodies (black arrowheads indicate a non-specific band recognised by the mCherry antibody; white arrowheads indicate the IAA-tFT proteins). The lower panels show Ponceau S staining following transfer and positions of molecular weight markers (kDa) are indicated to the left.

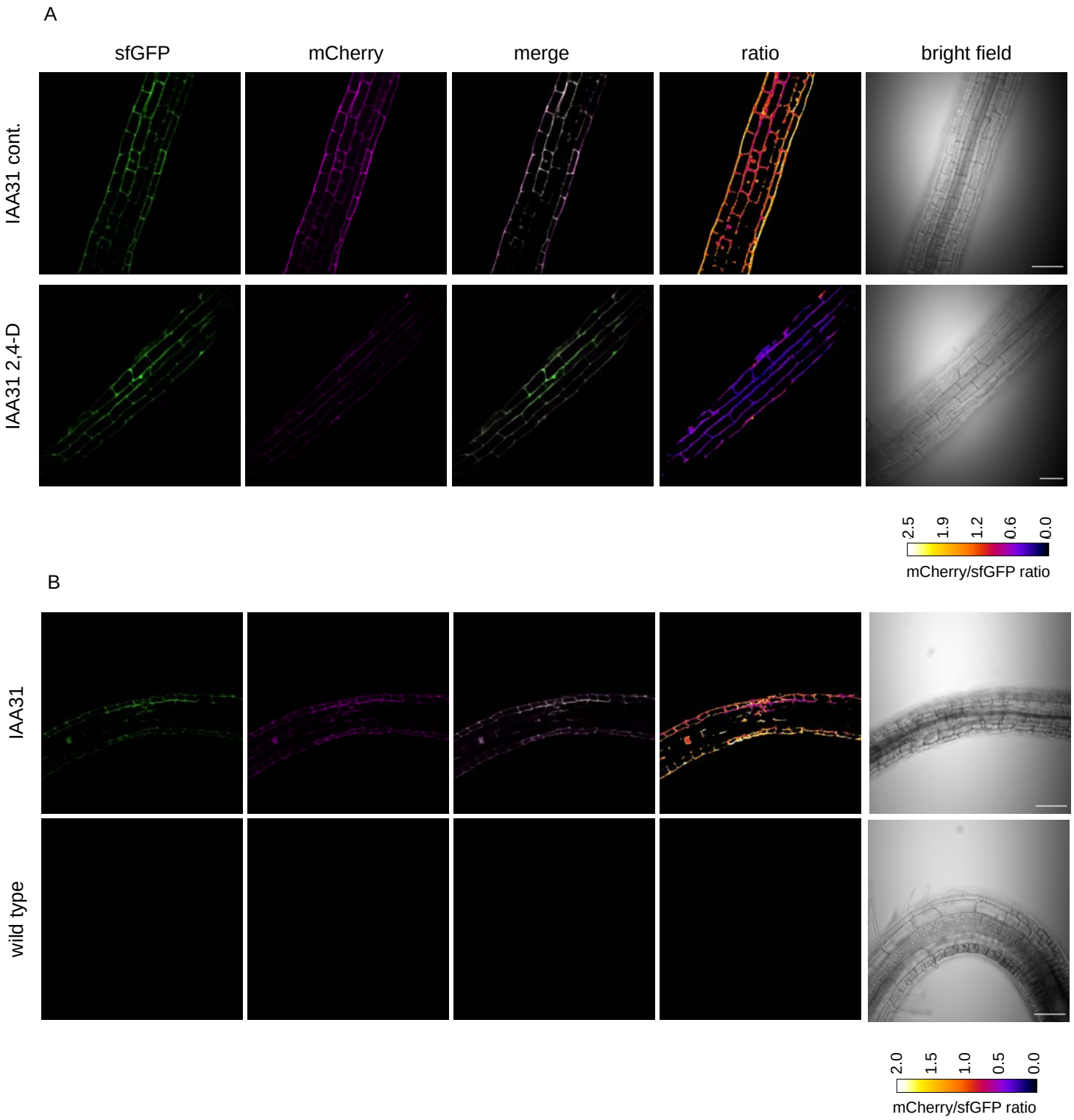

Figure 7 Auxin destabilises IAA31-tFT *in planta*
A, Confocal micrographs of primary roots of 6 d-old IAA31-tFT seedlings, treated with 5 μM 2,4-D or ethanol (cont.) for 4 h. B, Confocal micrographs of 14 d-old IAA31-tFT roots turned for 16 h by 180° to induce root bending. Bar: 50 μm.

Parsed Citations

Abel S, Oeller PW, Theologis A (1994) Early auxin-induced genes encode short-lived nuclear proteins. Proc Natl Acad Sci U S A 91: 326-330

Pubmed: Author and Title
Google Scholar: Author Only Title Only Author and Title

Alber AB, Paquet ER, Biserni M, Naef F, Suter DM (2018) Single Live Cell Monitoring of Protein Turnover Reveals Intercellular Variability and Cell-Cycle Dependence of Degradation Rates. Mol Cell 71: 1079-1091 e1079

Pubmed: Author and Title
Google Scholar: Author Only Title Only Author and Title

Arase F, Nishitani H, Egusa M, Nishimoto N, Sakurai S, Sakamoto N, Kaminaka H (2012) IAA8 involved in lateral root formation interacts with the TIR1 auxin receptor and ARF transcription factors in Arabidopsis. PLoS One 7: e43414

Pubmed: Author and Title
Google Scholar: Author Only Title Only Author and Title

Bachmair A, Finley D, Varshavsky A (1986) In vivo half-life of a protein is a function of its amino-terminal residue. Science 234: 179-186

Pubmed: Author and Title
Google Scholar: Author Only Title Only Author and Title

Barry JD, Dona E, Gilmour D, Huber W (2016) TimerQuant: a modelling approach to tandem fluorescent timer design and data interpretation for measuring protein turnover in embryos. Development 143: 174-179

Pubmed: Author and Title
Google Scholar: Author Only Title Only Author and Title

Bensimon A, Heck AJ, Aebersold R (2012) Mass spectrometry-based proteomics and network biology. Annu Rev Biochem 81: 379-405

Pubmed: Author and Title
Google Scholar: Author Only Title Only Author and Title

Boisvert FM, Ahmad Y, Gierlinski M, Charriere F, Lamont D, Scott M, Barton G, Lamond AI (2012) A quantitative spatial proteomics analysis of proteome turnover in human cells. Mol Cell Proteomics 11: M111 011429

Pubmed: Author and Title
Google Scholar: Author Only Title Only Author and Title

Brunoud G, Wells DM, Oliva M, Larrieu A, Mirabet V, Burrow AH, Beeckman T, Kepinski S, Traas J, Bennett MJ, Vernoux T (2012) A novel sensor to map auxin response and distribution at high spatio-temporal resolution. Nature 482: 103-106

Pubmed: Author and Title
Google Scholar: Author Only Title Only Author and Title

Calderón Villalobos LI, Lee S, De Oliveira C, Ivetac A, Brandt W, Armitage L, Sheard LB, Tan X, Parry G, Mao H, Zheng N, Napier R, Kepinski S, Estelle M (2012) A combinatorial TIR1/AFB-Aux/IAA co-receptor system for differential sensing of auxin. Nat Chem Biol 8: 477-485

Pubmed: Author and Title
Google Scholar: Author Only Title Only Author and Title

Ciechanover A (2013) Intracellular protein degradation: from a vague idea through the lysosome and the ubiquitin-proteasome system and onto human diseases and drug targeting. Bioorg Med Chem 21: 3400-3410

Pubmed: Author and Title
Google Scholar: Author Only Title Only Author and Title

Claydon AJ, Beynon R (2012) Proteome dynamics: revisiting turnover with a global perspective. Mol Cell Proteomics 11: 1551-1565

Pubmed: Author and Title
Google Scholar: Author Only Title Only Author and Title

De Rybel B, Vassileva V, Parizot B, Demeulenaere M, Grunewald W, Audenaert D, Van Campenhout J, Overvoorde P, Jansen L, Vanneste S, Möller B, Wilson M, Holman T, Van Isterdael G, Brunoud G, Vuylsteke M, Vernoux T, De Veylder L, Inzé D, Weijers D, Bennett MJ, Beeckman T (2010) A Novel Aux/IAA28 Signaling Cascade Activates GATA23-Dependent Specification of Lateral Root Founder Cell Identity. Current Biology 20: 1697-1706

Pubmed: Author and Title
Google Scholar: Author Only Title Only Author and Title

Dharmasiri N, Dharmasiri S, Estelle M (2005a) The F-box protein TIR1 is an auxin receptor. Nature 435: 441-445

Pubmed: Author and Title
Google Scholar: Author Only Title Only Author and Title

Dharmasiri N, Dharmasiri S, Weijers D, Lechner E, Yamada M, Hobbie L, Ehrismann JS, Jurgens G, Estelle M (2005b) Plant development is regulated by a family of auxin receptor F box proteins. Dev Cell 9: 109-119

Pubmed: Author and Title
Google Scholar: Author Only Title Only Author and Title

Doherty MK, Hammond DE, Clague MJ, Gaskell SJ, Beynon RJ (2009) Turnover of the human proteome: determination of protein intracellular stability by dynamic SILAC. J Proteome Res 8: 104-112

Pubmed: Author and Title

Google Scholar: Author Only Title Only Author and Title

Dona E, Barry JD, Valentin G, Quirin C, Khmelinskii A, Kunze A, Durdu S, Newton LR, Fernandez-Minan A, Huber W, Knop M, Gilmour D (2013) Directional tissue migration through a self-generated chemokine gradient. Nature 503: 285-289
Pubmed: Author and Title
Google Scholar: Author Only Title Only Author and Title

Dreher KA, Brown J, Saw RE, Callis J (2006) The Arabidopsis Aux/IAA protein family has diversified in degradation and auxin responsiveness. Plant Cell 18: 699-714
Pubmed: Author and Title
Google Scholar: Author Only Title Only Author and Title

Durrieu L, Kirrmaier D, Schneidt T, Kats I, Raghavan S, Hufnagel L, Saunders TE, Knop M (2018) Bicoid gradient formation mechanism and dynamics revealed by protein lifetime analysis. Molecular systems biology 14: e8355-e8355
Pubmed: Author and Title
Google Scholar: Author Only Title Only Author and Title

Eden E, Geva-Zatorsky N, Issaeva I, Cohen A, Dekel E, Danon T, Cohen L, Mayo A, Alon U (2011) Proteome half-life dynamics in living human cells. Science 331: 764-768
Pubmed: Author and Title
Google Scholar: Author Only Title Only Author and Title

Friml J (2010) Subcellular trafficking of PIN auxin efflux carriers in auxin transport. Eur J Cell Biol 89: 231-235
Pubmed: Author and Title
Google Scholar: Author Only Title Only Author and Title

Gallagher KL, Sozzani R, Lee CM (2014) Intercellular protein movement: deciphering the language of development. Annu Rev Cell Dev Biol 30: 207-233
Pubmed: Author and Title
Google Scholar: Author Only Title Only Author and Title

Garzón M, Eifler K, Faust A, Scheel H, Hofmann K, Koncz C, Yephremov A, Bachmair A (2007) PRT6/At5g02310 encodes an Arabidopsis ubiquitin ligase of the N-end rule pathway with arginine specificity and is not the CER3 locus. FEBS Lett 581: 3189-3196
Pubmed: Author and Title
Google Scholar: Author Only Title Only Author and Title

Gibbs DJ, Bacardit J, Bachmair A, Holdsworth MJ (2014) The eukaryotic N-end rule pathway: conserved mechanisms and diverse functions. Trends Cell Biol 24: 603-611
Pubmed: Author and Title
Google Scholar: Author Only Title Only Author and Title

Gibbs DJ, Bailey M, Tedds HM, Holdsworth MJ (2016) From start to finish: amino-terminal protein modifications as degradation signals in plants. New Phytol 211: 1188-1194
Pubmed: Author and Title
Google Scholar: Author Only Title Only Author and Title

Gibbs DJ, Lee SC, Isa NM, Gramuglia S, Fukao T, Bassel GW, Correia CS, Corbineau F, Theodoulou FL, Bailey-Serres J, Holdsworth MJ (2011) Homeostatic response to hypoxia is regulated by the N-end rule pathway in plants. Nature 479: 415-418
Pubmed: Author and Title
Google Scholar: Author Only Title Only Author and Title

Graciet E, Walter F, Maoileidigh DO, Pollmann S, Meyerowitz EM, Varshavsky A, Wellmer F (2009) The N-end rule pathway controls multiple functions during Arabidopsis shoot and leaf development. Proc Natl Acad Sci U S A 106: 13618-13623
Pubmed: Author and Title
Google Scholar: Author Only Title Only Author and Title

Gray WM, Kepinski S, Rouse D, Leyser O, Estelle M (2001) Auxin regulates SCF(TIR1)-dependent degradation of AUX/IAA proteins. Nature 414: 271-276
Pubmed: Author and Title
Google Scholar: Author Only Title Only Author and Title

Gross LA, Baird GS, Hoffman RC, Baldridge KK, Tsien RY (2000) The structure of the chromophore within DsRed, a red fluorescent protein from coral. PNAS 97: 11990-11995
Pubmed: Author and Title
Google Scholar: Author Only Title Only Author and Title

Habets ME, Offringa R (2014) PIN-driven polar auxin transport in plant developmental plasticity: a key target for environmental and endogenous signals. New Phytol 203: 362-377
Pubmed: Author and Title
Google Scholar: Author Only Title Only Author and Title

Holman SW, Hammond DE, Simpson DM, Waters J, Hurst JL, Beynon RJ (2016) Protein turnover measurement using selected reaction monitoring-mass spectrometry (SRM-MS). Philos Trans A Math Phys Eng Sci 374
Pubmed: Author and Title
Google Scholar: Author Only Title Only Author and Title

Hua Z, Vierstra RD (2011) The cullin-RING ubiquitin-protein ligases. Annu Rev Plant Biol 62: 299-334
Pubmed: Author and Title
Google Scholar: Author Only Title Only Author and Title

Hwang CS, Shemorry A, Varshavsky A (2010) N-terminal acetylation of cellular proteins creates specific degradation signals. Science 327: 973-977
Pubmed: Author and Title
Google Scholar: Author Only Title Only Author and Title

Karimi M, Bleys A, Vanderhaeghen R, Hilson P (2007) Building blocks for plant gene assembly. Plant Physiol 145: 1183-1191
Pubmed: Author and Title
Google Scholar: Author Only Title Only Author and Title

Karimi M, De Meyer B, Hilson P (2005) Modular cloning in plant cells. Trends Plant Sci 10: 103-105
Pubmed: Author and Title
Google Scholar: Author Only Title Only Author and Title

Kats I, Khmelinskii A, Kschonsak M, Huber F, Kniess RA, Bartosik A, Knop M (2018) Mapping Degradation Signals and Pathways in a Eukaryotic N-terminome. Mol Cell 70: 488-501 e485
Pubmed: Author and Title
Google Scholar: Author Only Title Only Author and Title

Kepinski S, Leyser O (2005) The Arabidopsis F-box protein TIR1 is an auxin receptor. Nature 435: 446-451
Pubmed: Author and Title
Google Scholar: Author Only Title Only Author and Title

Khmelinskii A, Keller PJ, Bartosik A, Meurer M, Barry JD, Mardin BR, Kaufmann A, Trautmann S, Wachsmuth M, Pereira G, Huber W, Schiebel E, Knop M (2012) Tandem fluorescent protein timers for in vivo analysis of protein dynamics. Nat Biotechnol 30: 708-714
Pubmed: Author and Title
Google Scholar: Author Only Title Only Author and Title

Khmelinskii A, Knop M (2014) Analysis of protein dynamics with tandem fluorescent protein timers. Methods Mol Biol 1174: 195-210
Pubmed: Author and Title
Google Scholar: Author Only Title Only Author and Title

Khmelinskii A, Meurer M, Ho CT, Besenbeck B, Fuller J, Lemberg MK, Bukau B, Mogk A, Knop M (2016) Incomplete proteasomal degradation of green fluorescent proteins in the context of tandem fluorescent protein timers. Mol Biol Cell 27: 360-370
Pubmed: Author and Title
Google Scholar: Author Only Title Only Author and Title

Knop M, Edgar BA (2014) Tracking protein turnover and degradation by microscopy: photo-switchable versus time-encoded fluorescent proteins. Open Biol 4: 140002
Pubmed: Author and Title
Google Scholar: Author Only Title Only Author and Title

Kraut DA, Israeli E, Schrader EK, Patil A, Nakai K, Nanavati D, Inobe T, Matouschek A (2012) Sequence- and species-dependence of proteasomal processivity. ACS Chem Biol 7: 1444-1453
Pubmed: Author and Title
Google Scholar: Author Only Title Only Author and Title

Kumar S, de Boer R, van der Klei IJ (2018) Yeast cells contain a heterogeneous population of peroxisomes that segregate asymmetrically during cell division. J Cell Sci 131
Pubmed: Author and Title
Google Scholar: Author Only Title Only Author and Title

Larrieu AP, French AP, Pridmore TP, Bennett MJ, Wells DM (2014) Time-profiling fluorescent reporters in the Arabidopsis root. Methods Mol Biol 1056: 11-17
Pubmed: Author and Title
Google Scholar: Author Only Title Only Author and Title

Laskowski M, Grieneisen VA, Hofhuis H, Hove CA, Hogeweg P, Maree AF, Scheres B (2008) Root system architecture from coupling cell shape to auxin transport. PLoS Biol 6: e307
Pubmed: Author and Title
Google Scholar: Author Only Title Only Author and Title

Lee JY, Colinas J, Wang JY, Mace D, Ohler U, Benfey PN (2006) Transcriptional and posttranscriptional regulation of transcription factor expression in Arabidopsis roots. Proc Natl Acad Sci U S A 103: 6055-6060
Pubmed: Author and Title
Google Scholar: Author Only Title Only Author and Title

Leyser HM, Pickett FB, Dharmasiri S, Estelle M (1996) Mutations in the AXR3 gene of Arabidopsis result in altered auxin response including ectopic expression from the SAUR-AC1 promoter. Plant J 10: 403-413
Pubmed: Author and Title
Google Scholar: Author Only Title Only Author and Title

Li L, Nelson CJ, Trosch J, Castleden I, Huang S, Millar AH (2017) Protein Degradation Rate in Arabidopsis thaliana Leaf Growth and Development. Plant Cell 29: 207-228
Pubmed: Author and Title
Google Scholar: Author Only Title Only Author and Title

Li X (2011) Infiltration of Nicotiana benthamiana Protocol for Transient Expression via Agrobacterium. Bio-protocol 1: e95
Pubmed: Author and Title
Google Scholar: Author Only Title Only Author and Title

Licausi F, Kosmacz M, Weits DA, Giuntoli B, Giorgi FM, Voesenek LA, Perata P, van Dongen JT (2011) Oxygen sensing in plants is mediated by an N-end rule pathway for protein destabilization. Nature 479: 419-422
Pubmed: Author and Title
Google Scholar: Author Only Title Only Author and Title

Linster E, Stephan I, Bienvenut WV, Maple-Grodem J, Myklebust LM, Huber M, Reichelt M, Sticht C, Geir Moller S, Meinnel T, Arnesen T, Giglione C, Hell R, Wirtz M (2015) Downregulation of N-terminal acetylation triggers ABA-mediated drought responses in Arabidopsis. Nat Commun 6: 7640
Pubmed: Author and Title
Google Scholar: Author Only Title Only Author and Title

Linster E, Wirtz M (2018) N-terminal acetylation: an essential protein modification emerges as an important regulator of stress responses. J Exp Bot 69: 4555-4568
Pubmed: Author and Title
Google Scholar: Author Only Title Only Author and Title

Long Y, Scheres B, Blilou I (2015) The logic of communication: roles for mobile transcription factors in plants. J Exp Bot 66: 1133-1144
Pubmed: Author and Title
Google Scholar: Author Only Title Only Author and Title

Mangano S, Gonzalez CD, Petruccelli S (2014) Agrobacterium tumefaciens-mediated transient transformation of Arabidopsis thaliana leaves. Methods Mol Biol 1062: 165-173
Pubmed: Author and Title
Google Scholar: Author Only Title Only Author and Title

Miricescu A, Goslin K, Graciet E (2018) Ubiquitylation in plants: signaling hub for the integration of environmental signals. J Exp Bot 69: 4511-4527
Pubmed: Author and Title
Google Scholar: Author Only Title Only Author and Title

Moss BL, Mao H, Guseman JM, Hinds TR, Hellmuth A, Kovenock M, Noorassa A, Lanctot A, Villalobos LI, Zheng N, Nemhauser JL (2015) Rate Motifs Tune Auxin/Indole-3-Acetic Acid Degradation Dynamics. Plant Physiol 169: 803-813
Pubmed: Author and Title
Google Scholar: Author Only Title Only Author and Title

Mot AC, Prell E, Klecker M, Naumann C, Faden F, Westermann B, Dissmeyer N (2018) Real-time detection of N-end rule-mediated ubiquitination via fluorescently labeled substrate probes. New Phytol 217: 613-624
Pubmed: Author and Title
Google Scholar: Author Only Title Only Author and Title

Nelson CJ, Li L, Jacoby RP, Millar AH (2013) Degradation rate of mitochondrial proteins in Arabidopsis thaliana cells. J Proteome Res 12: 3449-3459
Pubmed: Author and Title
Google Scholar: Author Only Title Only Author and Title

Nelson CJ, Li L, Millar AH (2014) Quantitative analysis of protein turnover in plants. Proteomics 14: 579-592
Pubmed: Author and Title
Google Scholar: Author Only Title Only Author and Title

Nelson CJ, Millar AH (2015) Protein turnover in plant biology. Nature Plants 1: 15017
Pubmed: Author and Title
Google Scholar: Author Only Title Only Author and Title

Ottenschläger I, Wolff P, Wolverton C, Bhalerao RP, Sandberg G, Ishikawa H, Evans M, Palme K (2003) Gravity-regulated differential auxin transport from columella to lateral root cap cells. Proc Natl Acad Sci U S A 100: 2987-2991
Pubmed: Author and Title
Google Scholar: Author Only Title Only Author and Title

Ouellet F, Overvoorde PJ, Theologis A (2001) IAA17/AXR3: Biochemical Insight into an Auxin Mutant Phenotype. Plant Cell 13: 829-841
Pubmed: Author and Title
Google Scholar: Author Only Title Only Author and Title

Podolec R, Ulm R (2018) Photoreceptor-mediated regulation of the COP1/SPA E3 ubiquitin ligase. Curr Opin Plant Biol 45: 18-25
Pubmed: Author and Title
Google Scholar: Author Only Title Only Author and Title

Potuschak T, Stary S, Schlogelhofer P, Becker F, Nejinskaia V, Bachmair A (1998) PRT1 of Arabidopsis thaliana encodes a component of the plant N-end rule pathway. Proc Natl Acad Sci U S A 95: 7904-7908
Pubmed: Author and Title
Google Scholar: Author Only Title Only Author and Title

Ramos JA, Zenser N, Leyser O, Callis J (2001) Rapid degradation of auxin/indoleacetic acid proteins requires conserved amino acids of domain II and is proteasome dependent. Plant Cell 13: 2349-2360
Pubmed: Author and Title
Google Scholar: Author Only Title Only Author and Title

Reed JW (2001) Roles and activities of Aux/IAA proteins in Arabidopsis. Trends Plant Sci 6: 420-425
Pubmed: Author and Title
Google Scholar: Author Only Title Only Author and Title

Rogg LE, Lasswell J, Bartel B (2001) A gain-of-function mutation in IAA28 suppresses lateral root development. Plant Cell 13: 465-480
Pubmed: Author and Title
Google Scholar: Author Only Title Only Author and Title

Rouse D, Mackay P, Stirnberg P, Estelle M, Leyser O (1998) Changes in auxin response from mutations in an AUX/IAA gene. Science 279: 1371-1373
Pubmed: Author and Title
Google Scholar: Author Only Title Only Author and Title

Sato A, Yamamoto KT (2008) Overexpression of the non-canonical Aux/IAA genes causes auxin-related aberrant phenotypes in Arabidopsis. Physiol Plant 133: 397-405
Pubmed: Author and Title
Google Scholar: Author Only Title Only Author and Title

Sato EM, Hijazi H, Bennett MJ, Vissenberg K, Swarup R (2015) New insights into root gravitropic signalling. J Exp Bot 66: 2155-2165
Pubmed: Author and Title
Google Scholar: Author Only Title Only Author and Title

Savitski MM, Zinn N, Faelth-Savitski M, Poeckel D, Gade S, Becher I, Muelbaier M, Wagner AJ, Strohmer K, Werner T, Melchert S, Petretich M, Rutkowska A, Vappiani J, Franken H, Steidel M, Sweetman GM, Gilan O, Lam EYN, Dawson MA, Prinjha RK, Grandi P, Bergamini G, Bantscheff M (2018) Multiplexed Proteome Dynamics Profiling Reveals Mechanisms Controlling Protein Homeostasis. Cell 173: 260-274.e225
Pubmed: Author and Title
Google Scholar: Author Only Title Only Author and Title

Schwanhäusser B, Busse D, Li N, Dittmar G, Schuchhardt J, Wolf J, Chen W, Selbach M (2011) Global quantification of mammalian gene expression control. Nature 473: 337-342
Pubmed: Author and Title
Google Scholar: Author Only Title Only Author and Title

Seibel NM, Eljouni J, Nalaskowski MM, Hampe W (2007) Nuclear localization of enhanced green fluorescent protein homomultimers. Anal Biochem 368: 95-99
Pubmed: Author and Title
Google Scholar: Author Only Title Only Author and Title

Shemiakina, II, Ermakova GV, Cranfill PJ, Baird MA, Evans RA, Souslova EA, Staroverov DB, Gorokhovatsky AY, Putintseva EV, Gorodnicheva TV, Chepurnykh TV, Strukova L, Lukyanov S, Zaraisky AG, Davidson MW, Chudakov DM, Shcherbo D (2012) A monomeric red fluorescent protein with low cytotoxicity. Nat Commun 3: 1204
Pubmed: Author and Title
Google Scholar: Author Only Title Only Author and Title

Sparkes IA, Runions J, Kearns A, Hawes C (2006) Rapid, transient expression of fluorescent fusion proteins in tobacco plants and generation of stably transformed plants. Nat Protoc 1: 2019-2025
Pubmed: Author and Title
Google Scholar: Author Only Title Only Author and Title

Stary S, Yin XJ, Potuschak T, Schlogelhofer P, Nizhynska V, Bachmair A (2003) PRT1 of Arabidopsis is a ubiquitin protein ligase of the plant N-end rule pathway with specificity for aromatic amino-terminal residues. Plant Physiol 133: 1360-1366
Pubmed: Author and Title
Google Scholar: Author Only Title Only Author and Title

Swarup R, Kramer EM, Perry P, Knox K, Leyser HM, Haseloff J, Beemster GT, Bhalerao R, Bennett MJ (2005) Root gravitropism requires lateral root cap and epidermal cells for transport and response to a mobile auxin signal. Nat Cell Biol 7: 1057-1065
Pubmed: Author and Title
Google Scholar: Author Only Title Only Author and Title

Tao LZ, Cheung AY, Nibau C, Wu HM (2005) RAC GTPases in tobacco and Arabidopsis mediate auxin-induced formation of proteolytically active nuclear protein bodies that contain AUX/IAA proteins. Plant Cell 17: 2369-2383
Pubmed: Author and Title
Google Scholar: Author Only Title Only Author and Title

Tian Q, Reed JW (1999) Control of auxin-regulated root development by the Arabidopsis thaliana SHY2/IAA3 gene. Development 126: 711-721
Pubmed: Author and Title
Google Scholar: Author Only Title Only Author and Title

Varshavsky A (2000) Ubiquitin fusion technique and its descendants. Methods Enzymol 327: 578-593
Pubmed: Author and Title
Google Scholar: Author Only Title Only Author and Title

Varshavsky A (2011) The N-end rule pathway and regulation by proteolysis. Protein Sci 20: 1298-1345
Pubmed: Author and Title
Google Scholar: Author Only Title Only Author and Title

Vicente J, Mendiondo GM, Movahedi M, Peirats-Llobet M, Juan Y-t, Shen Y-y, Dambire C, Smart K, Rodriguez PL, Charng Y-y, Gray JE, Holdsworth MJ (2017) The Cys-Arg/N-End Rule Pathway Is a General Sensor of Abiotic Stress in Flowering Plants. Current Biology 27: 3183-3190.e3184
Pubmed: Author and Title
Google Scholar: Author Only Title Only Author and Title

Vierstra RD (2009) The ubiquitin-26S proteasome system at the nexus of plant biology. Nat Rev Mol Cell Biol 10: 385-397
Pubmed: Author and Title
Google Scholar: Author Only Title Only Author and Title

Welle KA, Zhang T, Hryhorenko JR, Shen S, Qu J, Ghaemmaghami S (2016) Time-resolved Analysis of Proteome Dynamics by Tandem Mass Tags and Stable Isotope Labeling in Cell Culture (TMT-SILAC) Hyperplexing. Mol Cell Proteomics 15: 3551-3563
Pubmed: Author and Title
Google Scholar: Author Only Title Only Author and Title

Wirtz M, Birke H, Heeg C, Mueller C, Hosp F, Throm C, Koenig S, Feldman-Salit A, Rippe K, Petersen G, Wade RC, Rybin V, Scheffzek K, Hell R (2010) Structure and function of the hetero-oligomeric cysteine synthase complex in plants. J Biol Chem 285: 32810-32817
Pubmed: Author and Title
Google Scholar: Author Only Title Only Author and Title

Worley CK, Zenser N, Ramos J, Rouse D, Leyser O, Theologis A, Callis J (2000) Degradation of Aux/IAA proteins is essential for normal auxin signalling. Plant J 21: 553-562
Pubmed: Author and Title
Google Scholar: Author Only Title Only Author and Title

Xu F, Huang Y, Li L, Gannon P, Linster E, Huber M, Kapos P, Bienvenut W, Polevoda B, Meinnel T, Hell R, Giglione C, Zhang Y, Wirtz M, Chen S, Li X (2015) Two N-terminal acetyltransferases antagonistically regulate the stability of a nod-like receptor in Arabidopsis. Plant Cell 27: 1547-1562
Pubmed: Author and Title
Google Scholar: Author Only Title Only Author and Title

Zanetti ME, Chang IF, Gong F, Galbraith DW, Bailey-Serres J (2005) Immunopurification of polyribosomal complexes of Arabidopsis for global analysis of gene expression. Plant Physiol 138: 624-635
Pubmed: Author and Title
Google Scholar: Author Only Title Only Author and Title